Diffraction from magnetic materials

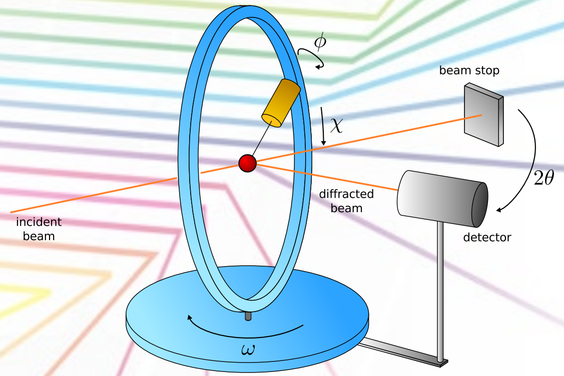

Navid Qureshi

Motivation

Impact of magnetic neutron scattering

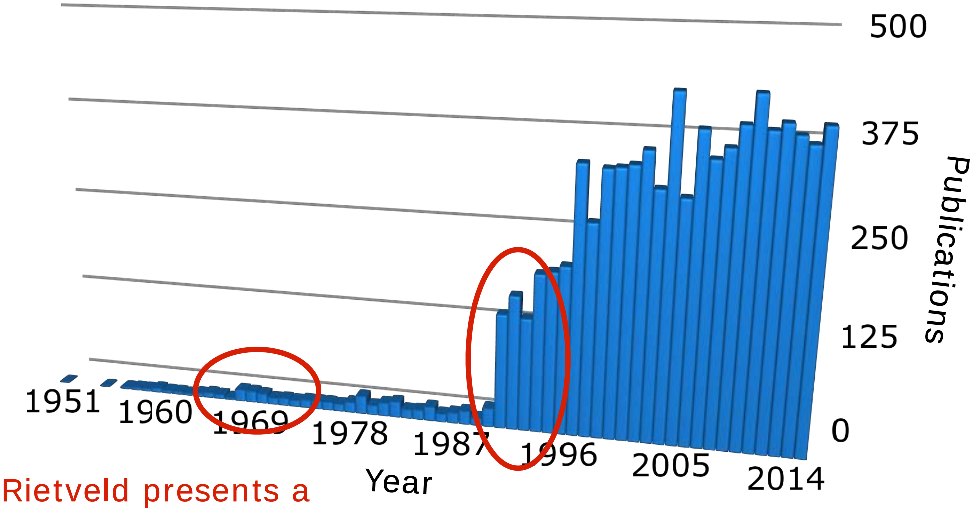

H. Rietveld presents a least-squares program able to refine crystal and magnetic structures

J. Rodríguez Carvajal presents the FullProf package

correlated with

- availability of computing tools
- relevant topics in new materials

Motivation

Impact of magnetic neutron scattering

1. A PROFILE REFINEMENT METHOD FOR NUCLEAR AND MAGNETIC STRUCTURES
By: RIETVELD, HM
JOURNAL OF APPLIED CRYSTALLOGRAPHY Volume: 2 Pages: 65-& Part: 2 Published: 1969
Full Text from Publisher
Times Cited: 9,132 (from All Databases)
Usage Count

2. RECENT ADVANCES IN MAGNETIC-STRUCTURE DETERMINATION BY NEUTRON POWDER DIFFRACTION
By: RODRIGUEZCARVAJAL, J
Conference: WORKSHOP ON THE USE OF NEUTRONS AND X-RAYS IN THE STUDY OF MAGNETISM Location: GRENOBLE, FRANCE Date: JAN 21-23, 1993
Sponsor(s): INST LAUE LANGEVIN; EUROPEAN SYNCHROTRON RADIAT FACIL
PHYSICA B Volume: 192 Issue: 1-2 Pages: 55-69 Published: OCT 1993
Full Text from Publisher | View Abstract
Times Cited: 5,680 (from All Databases)
Usage Count

3. Magnetic control of ferroelectric polarization
By: Kimura, T; Goto, T; Shintani, H; et al.
NATURE Volume: 426 Issue: 6962 Pages: 55-58 Published: NOV 6 2003
Full Text from Publisher | View Abstract
Times Cited: 2,423 (from All Databases)
Usage Count

4. Physics and Applications of Bismuth Ferrite
By: Catalan, Gustau; Scott, James F.
ADVANCED MATERIALS Volume: 21 Issue: 24 Pages: 2463-2485 Published: JUN 26 2009
Full Text from Publisher | View Abstract
Times Cited: 1,363 (from All Databases)
Highly Cited Paper
Usage Count

5. Magnetic order close to superconductivity in the iron-based layered LaO(1-x)F(x)FeAs systems
By: de la Cruz, Clarina; Huang, Q.; Lynn, J. W.; et al.
NATURE Volume: 453 Issue: 7197 Pages: 899-902 Published: JUN 12 2008
Full Text from Publisher | View Abstract
Times Cited: 1,347 (from All Databases)
Highly Cited Paper
Usage Count

6. Magnetic nanoparticles
By: Kodama, RH
JOURNAL OF MAGNETISM AND MAGNETIC MATERIALS Volume: 200 Issue: 1-3 Pages: 359-372 Published: OCT 1999
Full Text from Publisher | View Abstract
Times Cited: 934 (from All Databases)
Usage Count

7. Charge, orbital, and magnetic ordering in La0.5Ca0.5MnO3
By: Radaelli, PG; Cox, DE; Marezio, M; et al.
PHYSICAL REVIEW B Volume: 55 Issue: 5 Pages: 3015-3023 Published: FEB 1 1997
Full Text from Publisher | View Abstract
Times Cited: 741 (from All Databases)
Usage Count

correlated with

- availability of computing tools
- relevant topics in new materials

Motivation

Impact of magnetic neutron scattering

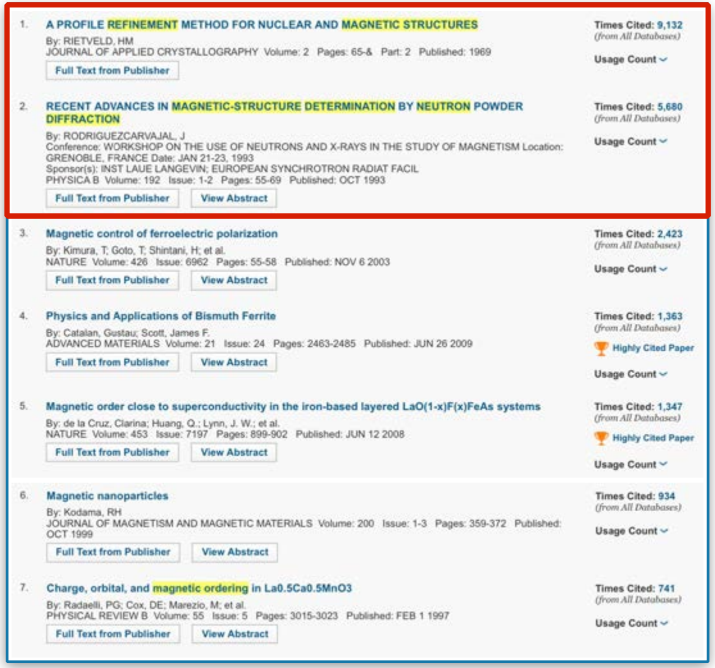
1. A PROFILE REFINEMENT METHOD FOR NUCLEAR AND MAGNETIC STRUCTURES
By: RIETVELD, HM
JOURNAL OF APPLIED CRYSTALLOGRAPHY Volume: 2 Pages: 65-& Part: 2 Published: 1969
Full Text from Publisher
Times Cited: 9,132 (from All Databases)
Usage Count

2. RECENT ADVANCES IN MAGNETIC-STRUCTURE DETERMINATION BY NEUTRON POWDER DIFFRACTION
By: RODRIGUEZCARVAJAL, J
Conference: WORKSHOP ON THE USE OF NEUTRONS AND X-RAYS IN THE STUDY OF MAGNETISM Location: GRENOBLE, FRANCE Date: JAN 21-23, 1993
Sponsor(s): INST LAUE LANGEVIN; EUROPEAN SYNCHROTRON RADIAT FACIL
PHYSICA B Volume: 192 Issue: 1-2 Pages: 55-69 Published: OCT 1993
Full Text from Publisher | View Abstract
Times Cited: 5,680 (from All Databases)
Usage Count

3. Magnetic control of ferroelectric polarization
By: Kimura, T; Goto, T; Shintani, H; et al.
NATURE Volume: 426 Issue: 6962 Pages: 55-58 Published: NOV 6 2003
Full Text from Publisher | View Abstract
Times Cited: 2,423 (from All Databases)
Usage Count

4. Physics and Applications of Bismuth Ferrite
By: Catalan, Gustau; Scott, James F.
ADVANCED MATERIALS Volume: 21 Issue: 24 Pages: 2463-2485 Published: JUN 26 2009
Full Text from Publisher | View Abstract
Times Cited: 1,363 (from All Databases)
Highly Cited Paper
Usage Count

5. Magnetic order close to superconductivity in the iron-based layered LaO(1-x)F(x)FeAs systems
By: de la Cruz, Clarina; Huang, Q.; Lynn, J. W.; et al.
NATURE Volume: 453 Issue: 7197 Pages: 899-902 Published: JUN 12 2008
Full Text from Publisher | View Abstract
Times Cited: 1,347 (from All Databases)
Highly Cited Paper
Usage Count

6. Magnetic nanoparticles
By: Kodama, RH
JOURNAL OF MAGNETISM AND MAGNETIC MATERIALS Volume: 200 Issue: 1-3 Pages: 359-372 Published: OCT 1999
Full Text from Publisher | View Abstract
Times Cited: 934 (from All Databases)
Usage Count

7. Charge, orbital, and magnetic ordering in La0.5Ca0.5MnO3
By: Radaelli, PG; Cox, DE; Marezio, M; et al.
PHYSICAL REVIEW B Volume: 55 Issue: 5 Pages: 3015-3023 Published: FEB 1 1997
Full Text from Publisher | View Abstract
Times Cited: 741 (from All Databases)
Usage Count

correlated with

- availability of computing tools
- relevant topics in new materials

Methods and computing programs

Motivation

Impact of magnetic neutron scattering

1. A PROFILE REFINEMENT METHOD FOR NUCLEAR AND MAGNETIC STRUCTURES
By: RIETVELD, HM
JOURNAL OF APPLIED CRYSTALLOGRAPHY Volume: 2 Pages: 65-& Part: 2 Published: 1969
Full Text from Publisher
Times Cited: 9,132 (from All Databases)
Usage Count

2. RECENT ADVANCES IN MAGNETIC-STRUCTURE DETERMINATION BY NEUTRON POWDER DIFFRACTION
By: RODRIGUEZCARVAJAL, J
Conference: WORKSHOP ON THE USE OF NEUTRONS AND X-RAYS IN THE STUDY OF MAGNETISM Location: GRENOBLE, FRANCE Date: JAN 21-23, 1993
Sponsor(s): INST LAUE LANGEVIN; EUROPEAN SYNCHROTRON RADIAT FACIL
PHYSICA B Volume: 192 Issue: 1-2 Pages: 55-69 Published: OCT 1993
Full Text from Publisher | View Abstract
Times Cited: 5,680 (from All Databases)
Usage Count

3. Magnetic control of ferroelectric polarization
By: Kimura, T; Goto, T; Shintani, H; et al.
NATURE Volume: 426 Issue: 6962 Pages: 55-58 Published: NOV 6 2003
Full Text from Publisher | View Abstract
Times Cited: 2,423 (from All Databases)
Usage Count

4. Physics and Applications of Bismuth Ferrite
By: Catalan, Gustau; Scott, James F.
ADVANCED MATERIALS Volume: 21 Issue: 24 Pages: 2463-2485 Published: JUN 26 2009
Full Text from Publisher | View Abstract
Times Cited: 1,363 (from All Databases)
Highly Cited Paper
Usage Count

5. Magnetic order close to superconductivity in the iron-based layered LaO(1-x)F(x)FeAs systems
By: de la Cruz, Clarina; Huang, Q.; Lynn, J. W.; et al.
NATURE Volume: 453 Issue: 7197 Pages: 899-902 Published: JUN 12 2008
Full Text from Publisher | View Abstract
Times Cited: 1,347 (from All Databases)
Highly Cited Paper
Usage Count

6. Magnetic nanoparticles
By: Kodama, RH
JOURNAL OF MAGNETISM AND MAGNETIC MATERIALS Volume: 200 Issue: 1-3 Pages: 359-372 Published: OCT 1999
Full Text from Publisher | View Abstract
Times Cited: 934 (from All Databases)
Usage Count

7. Charge, orbital, and magnetic ordering in La0.5Ca0.5MnO3
By: Radaelli, PG; Cox, DE; Marezio, M; et al.
PHYSICAL REVIEW B Volume: 55 Issue: 5 Pages: 3015-3023 Published: FEB 1 1997
Full Text from Publisher | View Abstract
Times Cited: 741 (from All Databases)
Usage Count

correlated with

- availability of computing tools
- relevant topics in new materials

Multiferroics

Motivation

Impact of magnetic neutron scattering

1. A PROFILE REFINEMENT METHOD FOR NUCLEAR AND MAGNETIC STRUCTURES
By: RIETVELD, HM
JOURNAL OF APPLIED CRYSTALLOGRAPHY Volume: 2 Pages: 65-& Part: 2 Published: 1969
Full Text from Publisher
Times Cited: 9,132 (from All Databases)
Usage Count

2. RECENT ADVANCES IN MAGNETIC-STRUCTURE DETERMINATION BY NEUTRON POWDER DIFFRACTION
By: RODRIGUEZCARVAJAL, J
Conference: WORKSHOP ON THE USE OF NEUTRONS AND X-RAYS IN THE STUDY OF MAGNETISM Location: GRENOBLE, FRANCE Date: JAN 21-23, 1993
Sponsor(s): INST LAUE LANGEVIN; EUROPEAN SYNCHROTRON RADIAT FACIL
PHYSICA B Volume: 192 Issue: 1-2 Pages: 55-69 Published: OCT 1993
Full Text from Publisher | View Abstract
Times Cited: 5,680 (from All Databases)
Usage Count

3. Magnetic control of ferroelectric polarization
By: Kimura, T; Goto, T; Shintani, H; et al.
NATURE Volume: 426 Issue: 6962 Pages: 55-58 Published: NOV 6 2003
Full Text from Publisher | View Abstract
Times Cited: 2,423 (from All Databases)
Usage Count

4. Physics and Applications of Bismuth Ferrite
By: Catalan, Gustau; Scott, James F.
ADVANCED MATERIALS Volume: 21 Issue: 24 Pages: 2463-2485 Published: JUN 26 2009
Full Text from Publisher | View Abstract
Times Cited: 1,363 (from All Databases)
Highly Cited Paper
Usage Count

5. Magnetic order close to superconductivity in the iron-based layered LaO(1-x)F(x)FeAs systems
By: de la Cruz, Clarina; Huang, Q.; Lynn, J. W.; et al.
NATURE Volume: 453 Issue: 7197 Pages: 899-902 Published: JUN 12 2008
Full Text from Publisher | View Abstract
Times Cited: 1,347 (from All Databases)
Highly Cited Paper
Usage Count

6. Magnetic nanoparticles
By: Kodama, RH
JOURNAL OF MAGNETISM AND MAGNETIC MATERIALS Volume: 200 Issue: 1-3 Pages: 359-372 Published: OCT 1999
Full Text from Publisher | View Abstract
Times Cited: 934 (from All Databases)
Usage Count

7. Charge, orbital, and magnetic ordering in La0.5Ca0.5MnO3
By: Radaelli, PG; Cox, DE; Marezio, M; et al.
PHYSICAL REVIEW B Volume: 55 Issue: 5 Pages: 3015-3023 Published: FEB 1 1997
Full Text from Publisher | View Abstract
Times Cited: 741 (from All Databases)
Usage Count

correlated with

- availability of computing tools
- relevant topics in new materials

Superconductors

Motivation

Impact of magnetic neutron scattering

1. A PROFILE REFINEMENT METHOD FOR NUCLEAR AND MAGNETIC STRUCTURES
By: RIETVELD, HM
JOURNAL OF APPLIED CRYSTALLOGRAPHY Volume: 2 Pages: 65-& Part: 2 Published: 1969
Full Text from Publisher
Times Cited: 9,132 (from All Databases)
Usage Count

2. RECENT ADVANCES IN MAGNETIC-STRUCTURE DETERMINATION BY NEUTRON POWDER DIFFRACTION
By: RODRIGUEZCARVAJAL, J
Conference: WORKSHOP ON THE USE OF NEUTRONS AND X-RAYS IN THE STUDY OF MAGNETISM Location: GRENOBLE, FRANCE Date: JAN 21-23, 1993
Sponsor(s): INST LAUE LANGEVIN; EUROPEAN SYNCHROTRON RADIAT FACIL
PHYSICA B Volume: 192 Issue: 1-2 Pages: 55-69 Published: OCT 1993
Full Text from Publisher | View Abstract
Times Cited: 5,680 (from All Databases)
Usage Count

3. Magnetic control of ferroelectric polarization
By: Kimura, T; Goto, T; Shintani, H; et al.
NATURE Volume: 426 Issue: 6962 Pages: 55-58 Published: NOV 6 2003
Full Text from Publisher | View Abstract
Times Cited: 2,423 (from All Databases)
Usage Count

4. Physics and Applications of Bismuth Ferrite
By: Catalan, Gustau; Scott, James F.
ADVANCED MATERIALS Volume: 21 Issue: 24 Pages: 2463-2485 Published: JUN 26 2009
Full Text from Publisher | View Abstract
Times Cited: 1,363 (from All Databases)
Highly Cited Paper
Usage Count

5. Magnetic order close to superconductivity in the iron-based layered LaO(1-x)F(x)FeAs systems
By: de la Cruz, Clarina; Huang, Q.; Lynn, J. W.; et al.
NATURE Volume: 453 Issue: 7197 Pages: 899-902 Published: JUN 12 2008
Full Text from Publisher | View Abstract
Times Cited: 1,347 (from All Databases)
Highly Cited Paper
Usage Count

6. Magnetic nanoparticles
By: Kodama, RH
JOURNAL OF MAGNETISM AND MAGNETIC MATERIALS Volume: 200 Issue: 1-3 Pages: 359-372 Published: OCT 1999
Full Text from Publisher | View Abstract
Times Cited: 934 (from All Databases)
Usage Count

7. Charge, orbital, and magnetic ordering in La0.5Ca0.5MnO3
By: Radaelli, PG; Cox, DE; Marezio, M; et al.
PHYSICAL REVIEW B Volume: 55 Issue: 5 Pages: 3015-3023 Published: FEB 1 1997
Full Text from Publisher | View Abstract
Times Cited: 741 (from All Databases)
Usage Count

correlated with

- availability of computing tools
- relevant topics in new materials

Nanoparticles

Motivation

Impact of magnetic neutron scattering

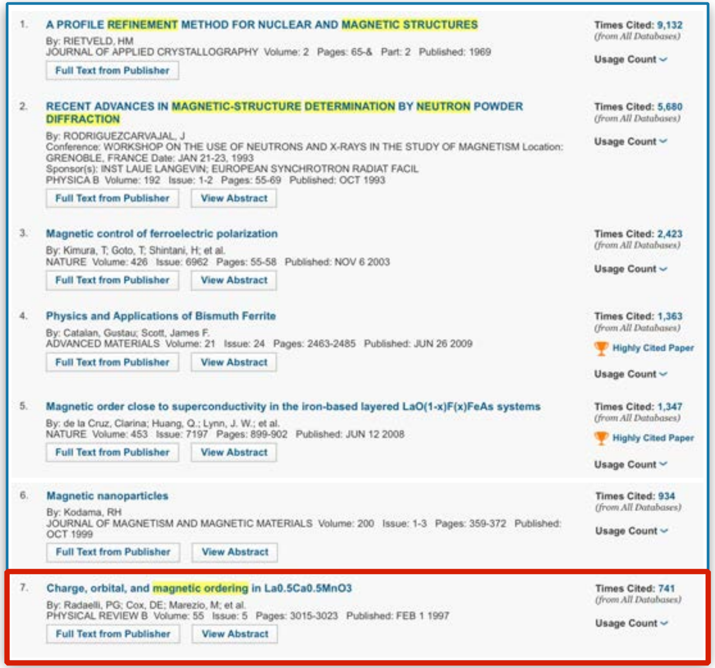

1. A PROFILE REFINEMENT METHOD FOR NUCLEAR AND MAGNETIC STRUCTURES
By: RIETVELD, HM
JOURNAL OF APPLIED CRYSTALLOGRAPHY Volume: 2 Pages: 65-& Part: 2 Published: 1969
Full Text from Publisher
Times Cited: 9,132 (from All Databases)
Usage Count

2. RECENT ADVANCES IN MAGNETIC-STRUCTURE DETERMINATION BY NEUTRON POWDER DIFFRACTION
By: RODRIGUEZCARVAJAL, J
Conference: WORKSHOP ON THE USE OF NEUTRONS AND X-RAYS IN THE STUDY OF MAGNETISM Location: GRENOBLE, FRANCE Date: JAN 21-23, 1993
Sponsor(s): INST LAUE LANGEVIN; EUROPEAN SYNCHROTRON RADIAT FACIL
PHYSICA B Volume: 192 Issue: 1-2 Pages: 55-69 Published: OCT 1993
Full Text from Publisher | View Abstract
Times Cited: 5,680 (from All Databases)
Usage Count

3. Magnetic control of ferroelectric polarization
By: Kimura, T; Goto, T; Shintani, H; et al.
NATURE Volume: 426 Issue: 6962 Pages: 55-58 Published: NOV 6 2003
Full Text from Publisher | View Abstract
Times Cited: 2,423 (from All Databases)
Usage Count

4. Physics and Applications of Bismuth Ferrite
By: Catalan, Gustau; Scott, James F.
ADVANCED MATERIALS Volume: 21 Issue: 24 Pages: 2463-2485 Published: JUN 26 2009
Full Text from Publisher | View Abstract
Times Cited: 1,363 (from All Databases)
Highly Cited Paper
Usage Count

5. Magnetic order close to superconductivity in the iron-based layered LaO(1-x)F(x)FeAs systems
By: de la Cruz, Clarina; Huang, Q.; Lynn, J. W.; et al.
NATURE Volume: 453 Issue: 7197 Pages: 899-902 Published: JUN 12 2008
Full Text from Publisher | View Abstract
Times Cited: 1,347 (from All Databases)
Highly Cited Paper
Usage Count

6. Magnetic nanoparticles
By: Kodama, RH
JOURNAL OF MAGNETISM AND MAGNETIC MATERIALS Volume: 200 Issue: 1-3 Pages: 359-372 Published: OCT 1999
Full Text from Publisher | View Abstract
Times Cited: 934 (from All Databases)
Usage Count

7. Charge, orbital, and magnetic ordering in La0.5Ca0.5MnO3
By: Radaelli, PG; Cox, DE; Marezio, M; et al.
PHYSICAL REVIEW B Volume: 55 Issue: 5 Pages: 3015-3023 Published: FEB 1 1997
Full Text from Publisher | View Abstract
Times Cited: 741 (from All Databases)
Usage Count

correlated with

- availability of computing tools
- relevant topics in new materials

Order phenomena in manganites

Outline

- Reminder: Nuclear scattering
  scattering amplitude, Fourier transform
- Magnetic scattering
  scattering potential, directional dependence
- Magnetic structures
  Ferro, antiferro, cycloids, helices, ...
- Scattering from a unit cell
  Magnetic structure factor, interaction vector
- Experimental procedure

Conventions for this lecture

Wave vector and scattering vector

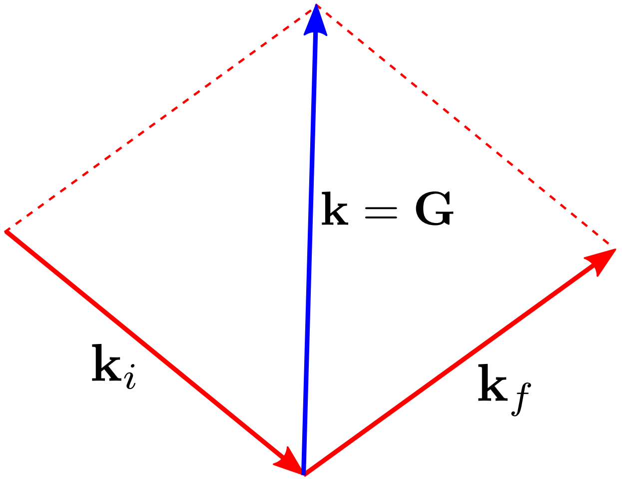

$\mathbf{k}_i$: initial wavevector

$\mathbf{k}_f$: final wavevector

$\mathbf{k}$: momentum transfer, scattering vector

$\mathbf{G}$: reciprocal lattice vector

Elastic scattering: $|\mathbf{k}_i| = |\mathbf{k}_f| = k$

Nuclear scattering

Scattering cross section

Number of neutrons *n* detected in solid angle Ω

$$\underbrace{dn}_{ns^{-1}} = \underbrace{\Phi}_{ncm^{-2}s^{-1}} \cdot \underbrace{d\Omega}_{1} \cdot \underbrace{\sigma(\theta,\varphi)}_{cm^2}$$

σ has the unit of a surface

usually in barns = 10^{-24} cm^2

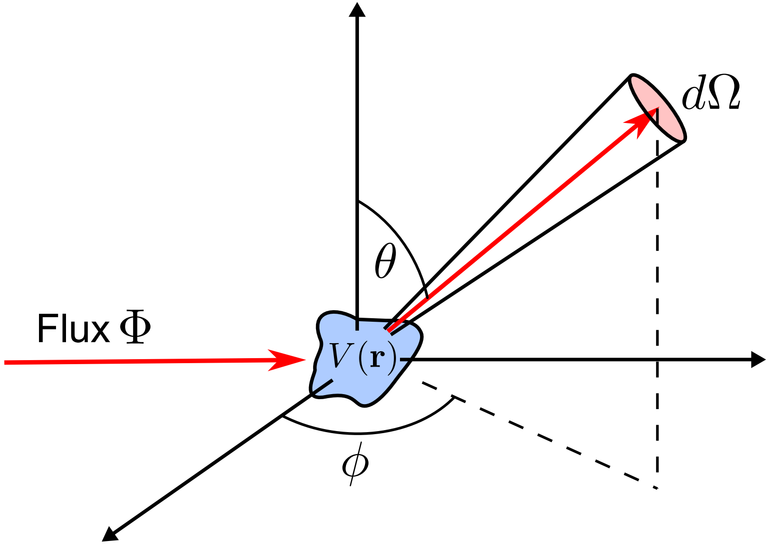

Nuclear scattering

Scattering cross section

The wave function at a spatial position **r** = sum of transmitted and scattered spherical wave function.

$$v_k^{scat}(\mathbf{r}) = e^{i\mathbf{kr}} + f_k(\theta, \varphi)\frac{e^{ikr}}{r}$$

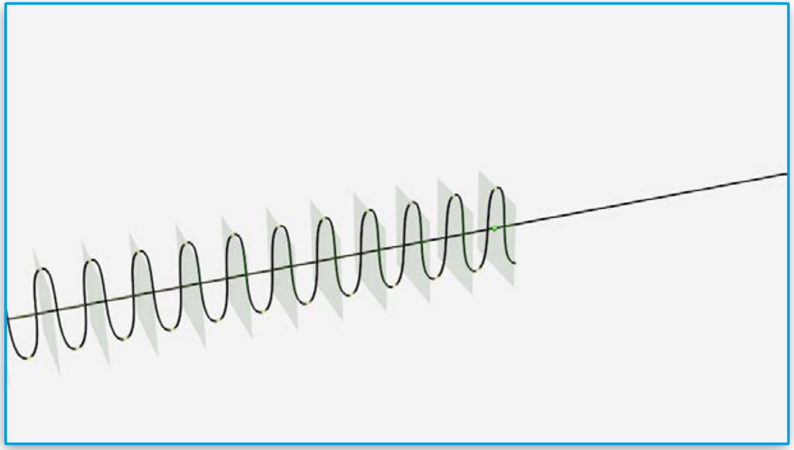

Only $f_k(\theta, \varphi)$ depends on the scattering potential $V(\mathbf{r})$.

Nuclear scattering

Scattering cross section

- mediated by strong force, short ranged (fm = 10^{-15} m)

- neutron wavelength much larger (10^{-10} m)
  → cannot probe internal structure
  → scattering is isotropic

- the interaction between the neutron and the atomic nucleus is represented by the Fermi pseudo-potential, a scalar field that is 0 except very close to the nucleus

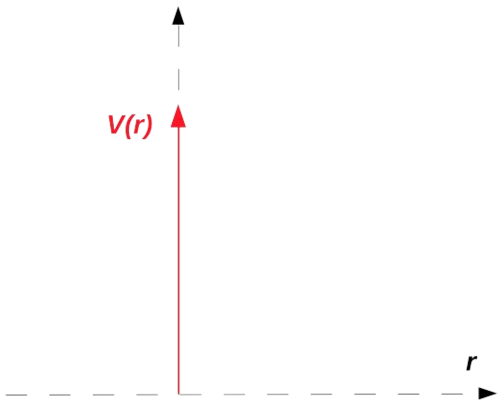

$$V(\mathbf{r}) = \frac{2\pi\hbar^2}{m_n} b\delta^3(\mathbf{r})$$

advantage: neutron senses atomic position and not the electron cloud (bonds)

Nuclear scattering

Scattering cross section

The scattering amplitude is related to the **Fourier transform of the potential function.**

$$f_k(\theta,\varphi) = -\frac{1}{4\pi}\frac{2\mu}{\hbar^2}\int V(\mathbf{r})e^{-i\mathbf{kr}}d^3\mathbf{r}$$

With the Fermi pseudo potential for neutron scattering from a nucleus $V(\mathbf{r}) = \frac{2\pi\hbar^2}{m_n} b\delta^3(\mathbf{r})$

$$|f_k(\theta,\varphi)| = b$$

Neutron scattering from a nucleus is isotropic!

b is in the order of 10^{-12} cm

Nuclear scattering

Comparison to X-rays

The amplitude of the scattered wave (the Fourier transform of the potential function) is called the atomic **form factor** *f* (X-rays) or **scattering length** *b* (neutrons).

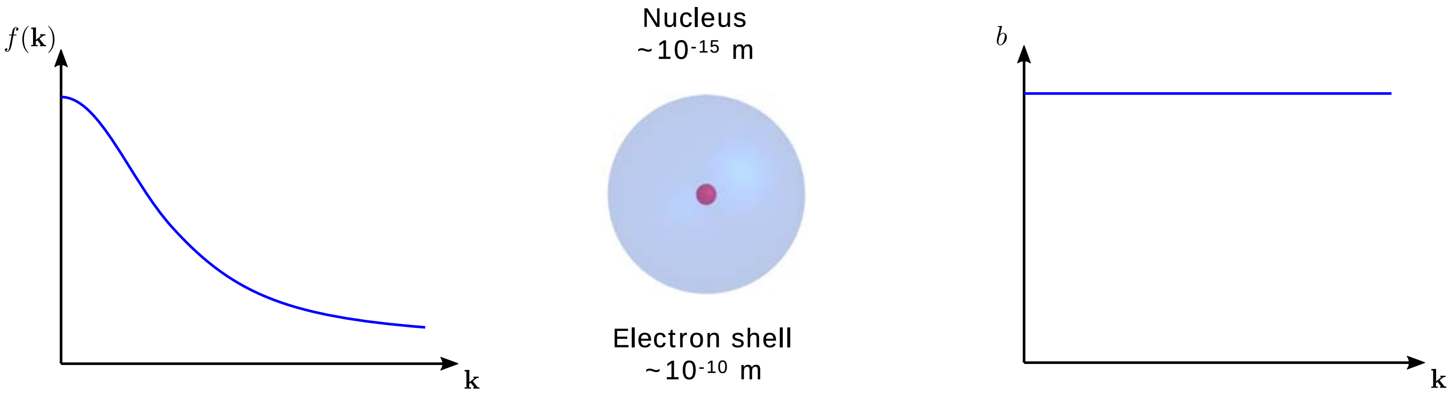

advantage with neutrons: scattered intensity does not drop with increasing scattering angle

Nuclear scattering

Comparison to X-rays

Scattering lengths (analog to X-ray form factor)

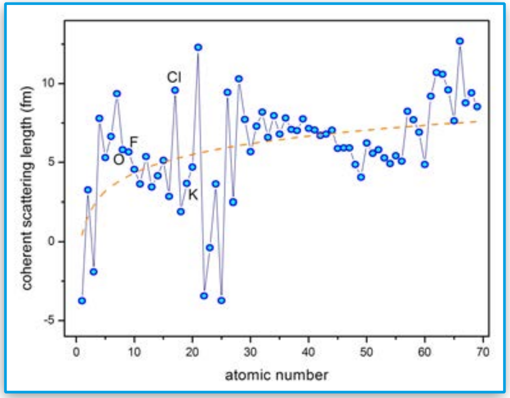

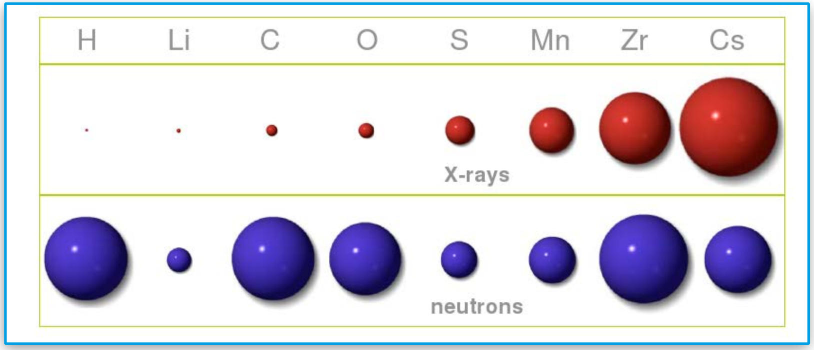

superposition of resonance scattering with slowly increasing potential scattering due to atomic weight

advantages: contrast between neighbouring elements
light elements can be measured easily
isotope effect (b_H=-3.7, b_D=6.8)

Nuclear scattering

Comparison to X-rays

Scattering lengths (analog to X-ray form factor)

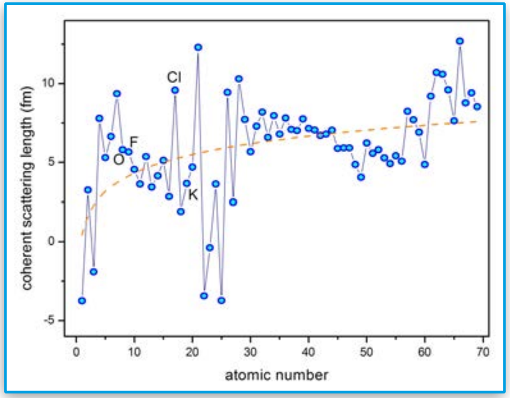

superposition of resonance scattering with slowly increasing potential scattering due to atomic weight

Example KCl:

scattering lengths of K and Cl are very different ⟶ strong contrast

X-rays would see a primitive cell with half the lattice constant

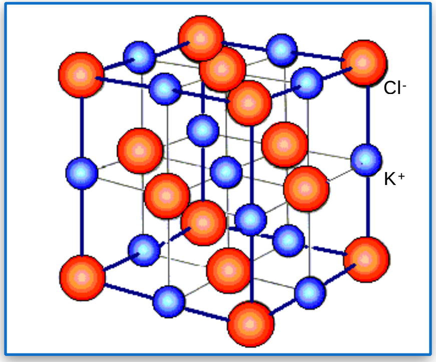

advantages: contrast between neighbouring elements

light elements can be measured easily

isotope effect (b_H=-3.7, b_D=6.8)

Magnetic scattering

Electron magnetic moment

Magnetic dipole moment in classical electrodynamics

$$\mu = I \cdot A$$

$$= \frac{-e \cdot v_e}{2\pi r} \cdot \pi r^2 = \frac{-e \cdot v_e}{2} \cdot r = \frac{-e}{2m} \cdot m v_e r = -\frac{e}{2m} L$$

Gyromagnetic ratio γ: ratio between magnetic dipole moment and total angular momentum

$$\gamma = -\frac{e}{2m} = -\frac{\mu_B}{\hbar} \quad \text{with} \quad \mu_B = \frac{e\hbar}{2m_e}$$

This works well for the electron's orbital momentum, but its intrinsic spin momentum cannot be explained in the classical approach ⟶ correction by g-factor

$$\gamma = -g_e \frac{\mu_B}{\hbar} \qquad (g_L = 1,\ g_S = 2)$$

Magnetic scattering

Electron magnetic moment

Angular momenta are quantised in units of $\hbar$ $(L = ..., -2\hbar, -\hbar, 0, \hbar, 2\hbar, ...)$

$$\gamma = -g_e \frac{\mu_B}{\hbar}$$ (g_L = 1, g_S = 2)

→ The magnetic moment of en electron is quantised in μ_B

$$\boldsymbol{\mu}_L = \gamma \mathbf{L} = -\frac{e}{2m_e}\mathbf{L} = -\mu_B \frac{\mathbf{L}}{\hbar}$$ orbital moment (1μ_B per $\hbar$)

Spin momenta are quantised in units of 1/2$\hbar$ $(S = ... -\frac{3}{2}\hbar, -\hbar, -\frac{1}{2}\hbar, 0, \frac{1}{2}\hbar, \hbar, \frac{3}{2}\hbar, ...)$

$$\boldsymbol{\mu}_S = \gamma \mathbf{S} = -\frac{e}{m_e}\mathbf{S} = -2\mu_B \frac{\mathbf{S}}{\hbar}$$ spin moment (1 μ_B per electron spin)

Total moment due to LS coupling $\mathbf{J} = \mathbf{L} + \mathbf{S}$: $\boldsymbol{\mu}_J = -g_J \mu_B \frac{\mathbf{J}}{\hbar}$

Magnetic scattering

Neutron magnetic moment

Protons, neutrons and many nuclei carry a nuclear spin.

Gyromagnetic ratios of common spin-1/2 particles:

Electron:	$1.76 \cdot 10^5$ MHz/T
Proton:	267 MHz/T
Neutron:	183 MHz/T

Neutron moment is around 960 times smaller than the electron moment.

		proton	neutron
Nuclear magnetons:	$\mu_N = \dfrac{e\hbar}{2m_p}$	$\mu_p = 2.793\,\mu_N$	$\mu_n = -1.913\,\mu_N$

For neutrons: $\boldsymbol{\mu}_n = \gamma \mu_N \boldsymbol{\sigma}$ with $\gamma_n = -1.913$

Magnetic scattering

Magnetic scattering potential

Magnetic scattering: interaction of the neutron spin with the magnetic field of an unpaired electron

neutron spin operator: $\hat{\boldsymbol{\mu}} = \gamma \mu_N \hat{\boldsymbol{\sigma}}$

gyromagnetic ratio $\gamma = -1.91$

nuclear magneton $\mu_N = \frac{m_e \mu_B}{m_n}$

Pauli spin operator $\hat{\boldsymbol{\sigma}}$

The interaction is described by the potential:

$$-\hat{\boldsymbol{\mu}} \cdot \mathbf{H} = -\gamma \mu_N \hat{\boldsymbol{\sigma}} \cdot \mathbf{H}$$

Magnetic scattering length proportional to electron radius $e^2/m_e c^2$:

$$\gamma r_0 = \frac{\gamma e^2}{m_e c^2} = -0.54 \cdot 10^{-12}\,\mathrm{cm}$$

→ comparable to nuclear scattering

Magnetic scattering

Magnetic scattering potential

Magnetic field due to a single electron moving with velocity $\mathbf{v}_e$:

$$\mathbf{H} = \mathrm{curl}\left(\frac{\boldsymbol{\mu}_e \times \mathbf{R}}{|\mathbf{R}|^3}\right) + \frac{-e}{c}\frac{\mathbf{v}_e \times \mathbf{R}}{|\mathbf{R}|^3}$$

(from S. W. Lovesey,
Theory of Neutron Scattering from
Condensed Matter, Volume 2)

The scattering cross section between the neutron and the electron becomes (after 2 pages):

$$\frac{\partial^2\sigma}{\partial\Omega\partial E} = r_0^2\frac{k_f}{k_i}\sum_{\alpha\beta}\left(\delta_{\alpha\beta} - \tilde{\mathbf{k}}_\alpha\tilde{\mathbf{k}}_\beta\right)\sum_{\lambda\lambda'} p_\lambda \langle\lambda|\tilde{\mathbf{k}}_\alpha^2|\lambda'\rangle\langle\lambda|\tilde{\mathbf{k}}_\beta^2|\lambda'\rangle\delta(\hbar\omega + E_\lambda - E_{\lambda'})$$

In comparison to nuclear scattering the magnetic cross section has a directional dependence!

Magnetic scattering

Magnetic scattering potential

Like for nuclear scattering the Born approximation holds and the scattered amplitude is the Fourier transformation of the potential function (atomic magnetisation density), the **magnetic form factor**.

$$f(\mathbf{k}) = \int \rho(\mathbf{r}) \exp(i\mathbf{k}\mathbf{r}) d\mathbf{r}$$

which is defined by:

$$f(\mathbf{k}) = \frac{g_S}{g} j_0(\mathbf{k}) + \frac{g_L}{g} \left[j_0(\mathbf{k}) + j_2(\mathbf{k}) \right]$$

g, g_L, g_S: g-factors

j_n: spherical Bessel functions

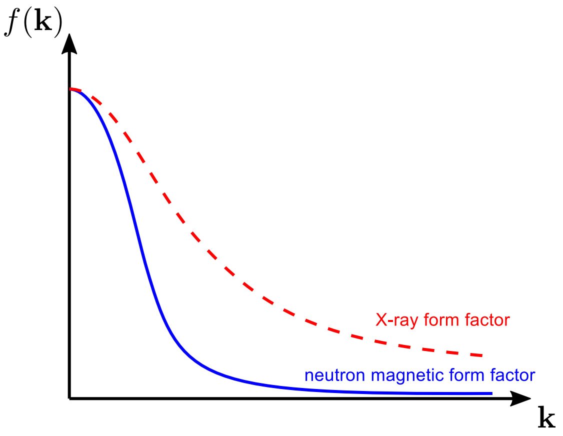

Magnetic scattering

Magnetic scattering potential

Like for nuclear scattering the Born approximation holds and the scattered amplitude is the Fourier transformation of the potential function (atomic magnetisation density), the **magnetic form factor**.

$$f(\mathbf{k}) = \int \rho(\mathbf{r}) \exp(i\mathbf{k}\mathbf{r}) d\mathbf{r}$$

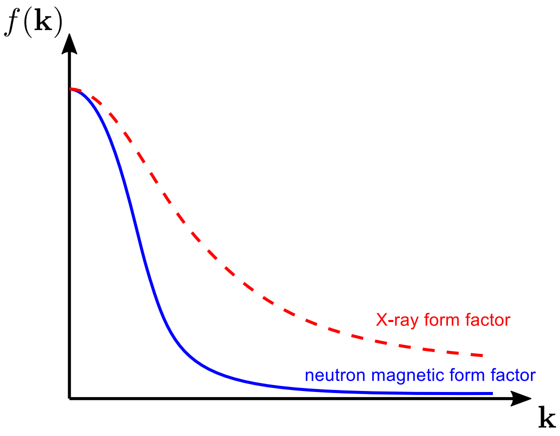

which is defined by:

$$f(\mathbf{k}) = \frac{g_S}{g} j_0(\mathbf{k}) + \frac{g_L}{g} \left[j_0(\mathbf{k}) + j_2(\mathbf{k}) \right]$$

g, g_L, g_S: g-factors

j_n: spherical Bessel functions

analytical approximation:

$$j_0(s) = A\exp(-as^2) + B\exp(-bs^2) + C\exp(-cs^2) + D$$

$$j_2(s) = \left[A\exp(-as^2) + B\exp(-bs^2) + C\exp(-cs^2) + D\right] \cdot s^2$$

$$s = \frac{\sin\theta}{\lambda}$$

coefficients a, A, b, B, c, C, D tabulated on http://www.ill.eu/sites/ccsl/html/ccsldoc.html)

Magnetic structures

Ordered magnetic state

In some crystals, some of the atoms/ions have unpaired electrons (transition metals, rare-earths).

Hund's rule favors a state with maximum S and L. The ions possess a localised magnetic moment.

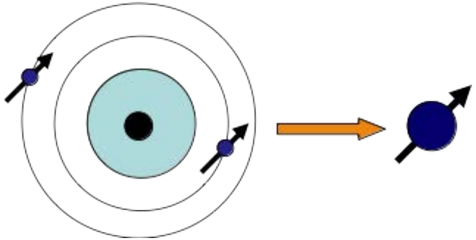

Exchange interactions (direct, superexchange, double exchange, RKKY, dipolar, ...) often stabilize a long-range magnetic order

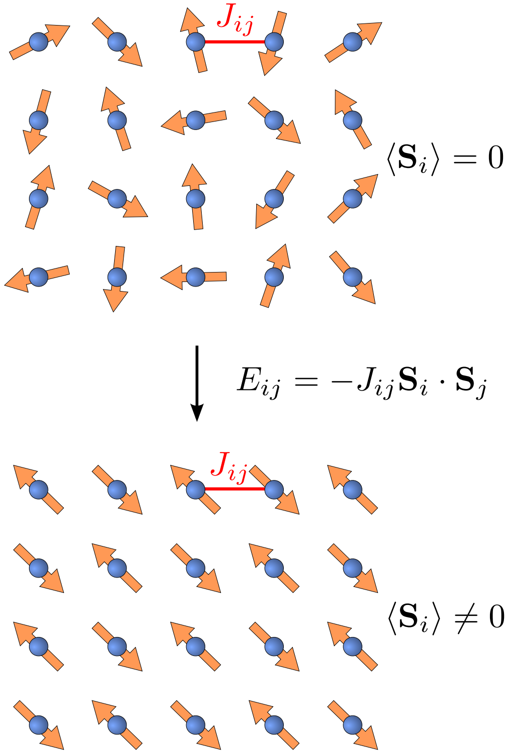

Magnetic structures

Propagation vector

The magnetic structure does not necessarily have the same periodicity and symmetry as the underlying crystal structure. The relation between one and another is expressed by the propagation or wave vector.

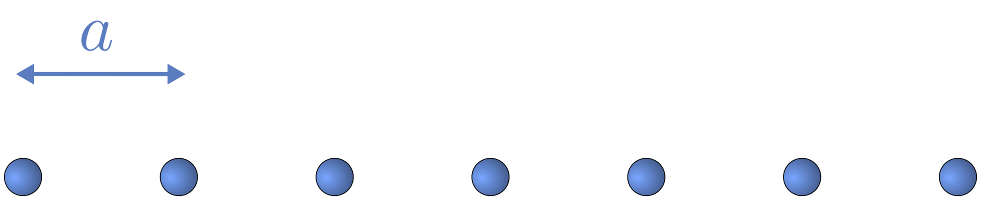

Magnetic structures

Propagation vector

The magnetic structure does not necessarily have the same periodicity and symmetry as the underlying crystal structure. The relation between one and another is expressed by the propagation or wave vector.

ferromagnetic

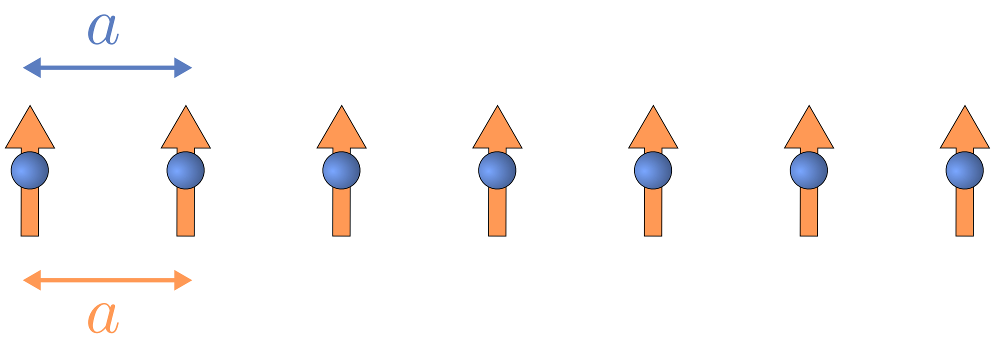

Magnetic structures

Propagation vector

The magnetic structure does not necessarily have the same periodicity and symmetry as the underlying crystal structure. The relation between one and another is expressed by the propagation or wave vector.

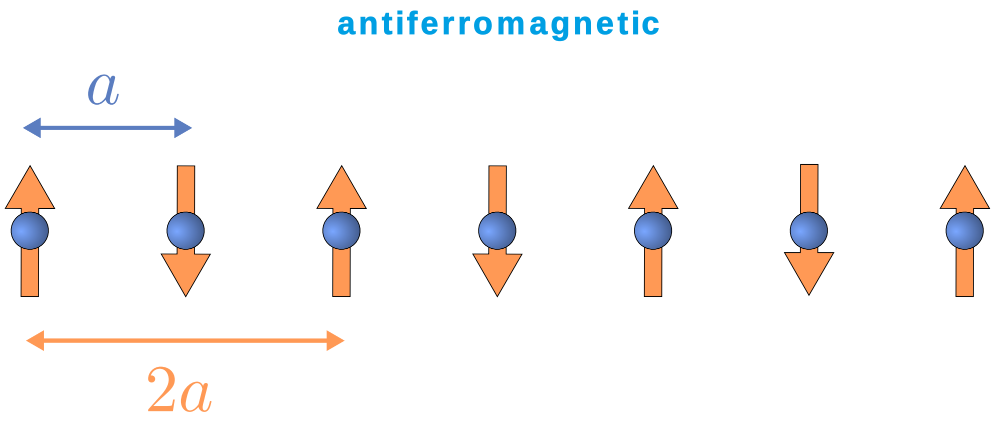

Magnetic structures

Propagation vector

The magnetic structure does not necessarily have the same periodicity and symmetry as the underlying crystal structure. The relation between one and another is expressed by the propagation or wave vector.

commensurate antiferromagnetic

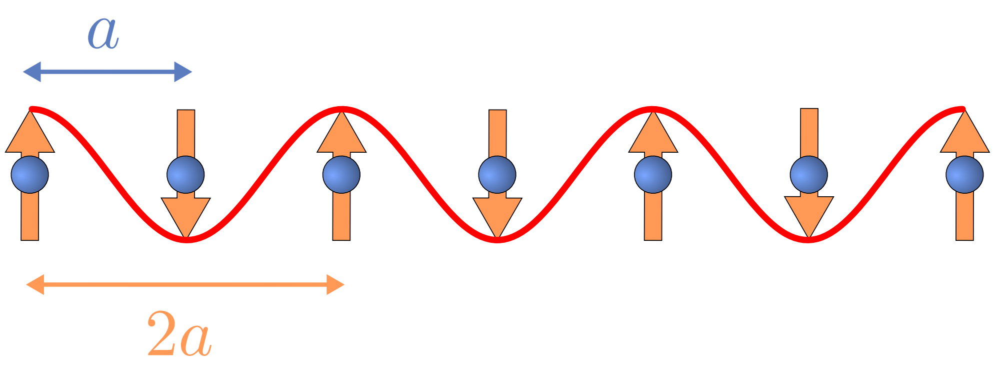

magnetic periodicity = 2 x nuclear periodicity $\rightarrow \mathbf{q} = (1/2\ 0\ 0)$

Magnetic structures

Propagation vector

The magnetic structure does not necessarily have the same periodicity and symmetry as the underlying crystal structure. The relation between one and another is expressed by the propagation or wave vector.

commensurate antiferromagnetic

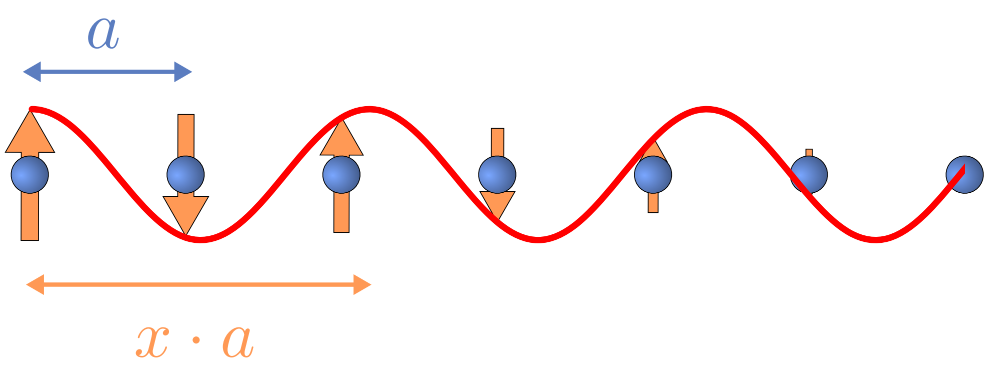

magnetic periodicity = x times nuclear periodicity $\rightarrow \mathbf{q} = (1/x\ 0\ 0)$

Magnetic structures

Propagation vector

Magnetic Bragg reflections can be found at $\mathbf{k} = \mathbf{G} \pm \mathbf{q}$

superposition for $\mathbf{q} = 0$ **Magnetic satellites for $\mathbf{q} \neq 0$**

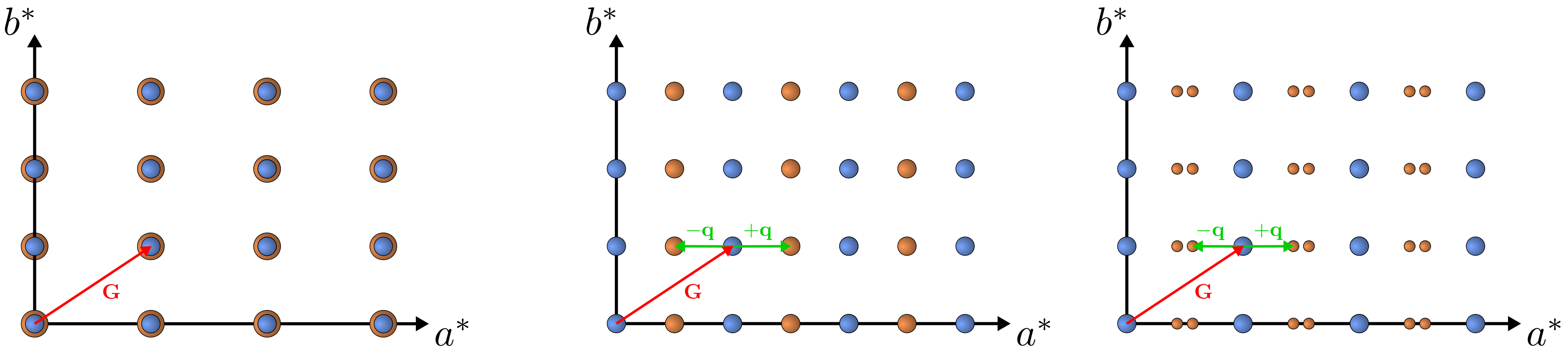

ferromagnetic

commensurate AF
$\mathbf{q} = (1/2\ 0\ 0)$

incommensurate AF
$\mathbf{q} = (1/2 - \delta\ 0\ 0)$

Magnetic structures

Fourier expansion of magnetic moments

One usually describes magnetic structures with Fourier components of the magnetic moments:

$$\boldsymbol{\mu}(\mathbf{r}) = \frac{1}{n_q}\sum_q \mathbf{S}_q \cdot e^{-i\mathbf{qr}}$$

which for a single propagation vector becomes:

$$\boldsymbol{\mu}(\mathbf{r}) = \frac{1}{2}(\mathbf{S}_q \cdot e^{-i\mathbf{qr}} + \mathbf{S}_{-q} \cdot e^{i\mathbf{qr}})$$

$\mathbf{S}_q$ is a complex vector made of linear combinations of basis vectors according to one or more irreducible representations.

Since $\boldsymbol{\mu}(\mathbf{r})$ is a real vector, one must impose the condition $\mathbf{S}^*_{-q} = \mathbf{S}_q$

Magnetic structures

Types of magnetic structures

q=0 ferromagnetic

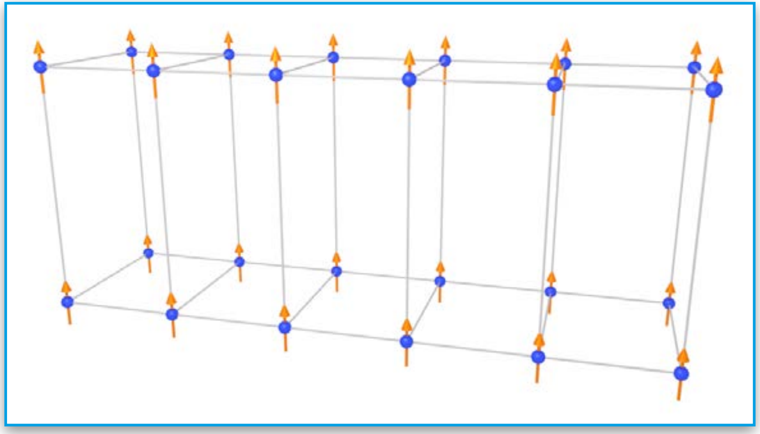

$$\boldsymbol{\mu}(\mathbf{r}) = \mathbf{S}_q \cdot e^{-i\mathbf{qr}} = \mathbf{S}_q$$

q=(100) antiferromagnetic (centered cells)

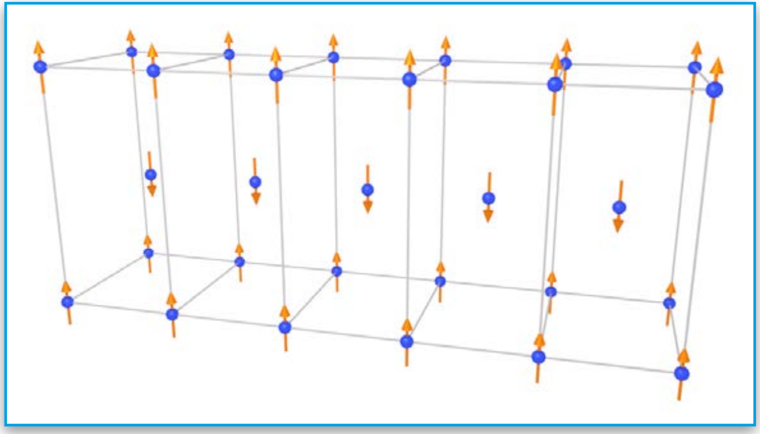

$$\boldsymbol{\mu}(\mathbf{r}) = \frac{1}{2}(\mathbf{S}_q \cdot e^{-i\mathbf{qr}} + \mathbf{S}_{-q} \cdot e^{i\mathbf{qr}}) = \mathbf{S}_q \cdot (-1)^{2r_x}$$

real Fourier components

Magnetic structures

Types of magnetic structures

antiferromagnetic, **q**=1/2**G** (at the border of the 1st Brillouin zone)

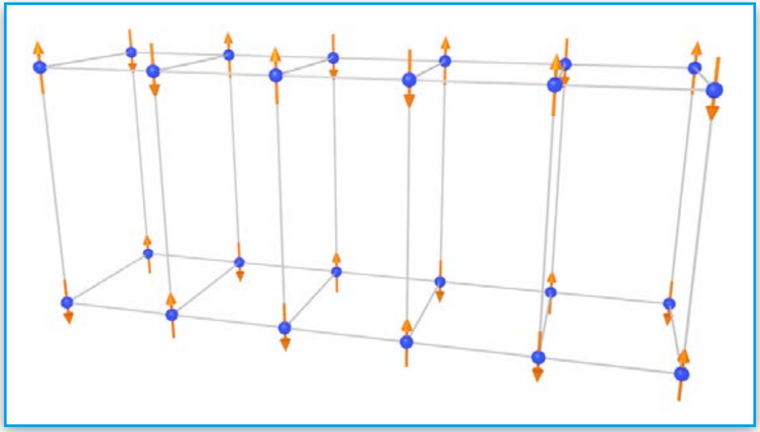

$$\boldsymbol{\mu}(\mathbf{r}) = \frac{1}{2}(\mathbf{S}_q \cdot e^{-i\mathbf{qr}} + \mathbf{S}_{-q} \cdot e^{i\mathbf{qr}}) = \mathbf{S}_q \cdot (-1)^{r_x}$$

real Fourier components

Magnetic structures

Types of magnetic structures

amplitude-modulated antiferromagnetic, **q**<1/2**G** (at the interior of the 1st Brillouin zone)

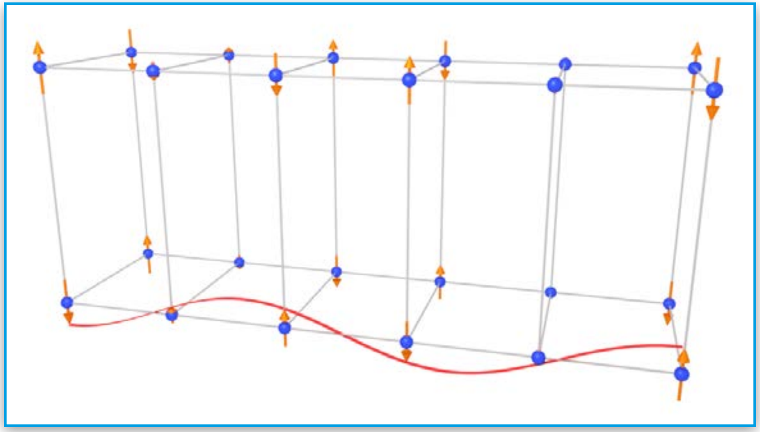

$$\mathbf{S}_q = \mu\hat{\mathbf{u}}e^{-i\mathbf{qr}} \qquad \boldsymbol{\mu}(\mathbf{r}) = \mu\hat{\mathbf{u}}\cos\left[2\pi(\mathbf{qr}+\phi_q)\right]$$

imaginary Fourier components (real and imaginary parts parallel)

Magnetic structures

Types of magnetic structures

antiferromagnetic spirals, **q**<1/2**G** (at the interior of the 1st Brillouin zone)

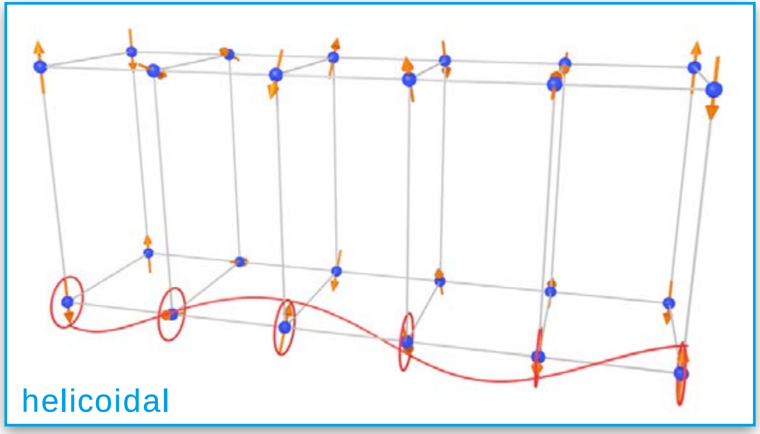

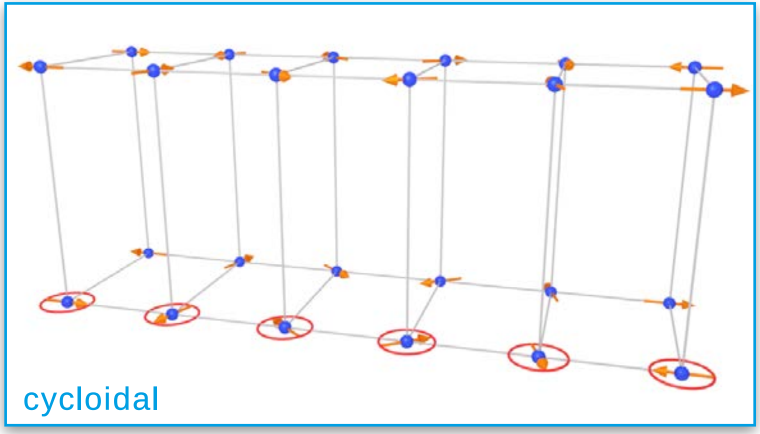

$$\mathbf{S}_q = (\mu_u \hat{\mathbf{u}} + i\mu_v \hat{\mathbf{v}})\, e^{-i\mathbf{qr}}$$

$$\boldsymbol{\mu}(\mathbf{r}) = \mu_u \hat{\mathbf{u}} \cos\left[2\pi(\mathbf{qr} + \phi_q)\right] + \mu_v \hat{\mathbf{v}} \sin\left[2\pi(\mathbf{qr} + \phi_q)\right]$$

imaginary Fourier components (real and imaginary parts perpendicular)

Magnetic structures

Types of magnetic structures

multi-**q** structures, e.g. conical (ferromagnetic **q**=0 component + helix)

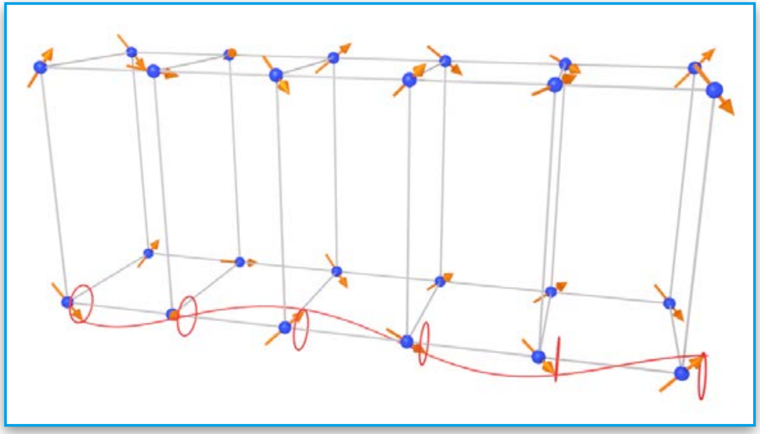

treatment of every component separately

Scattering from a unit cell

Reminder: Nuclear structure factor

imagine two scattering potentials (atoms), the first at 0, the second at **r**

The path difference is:

$$\Delta s(\mathbf{r}) = \mathbf{r}\cdot\frac{\mathbf{k}_f}{k_f} - \mathbf{r}\cdot\frac{\mathbf{k}_i}{k_i}$$

Therefore, the phase difference is:

$$\varphi(\mathbf{r}) = 2\pi\frac{\Delta s}{\lambda} = k\cdot\Delta s = (\mathbf{k}_f - \mathbf{k}_i)\cdot\mathbf{r} = \mathbf{G}\cdot\mathbf{r}$$

Sum up phase differences over atoms in unit cell:

$$F(hkl) = \sum_j b_j \exp(i\mathbf{G}\mathbf{r}_j) = \sum_j b_j \exp\left[2\pi i(hx_j + ky_j + lz_j)\right]$$

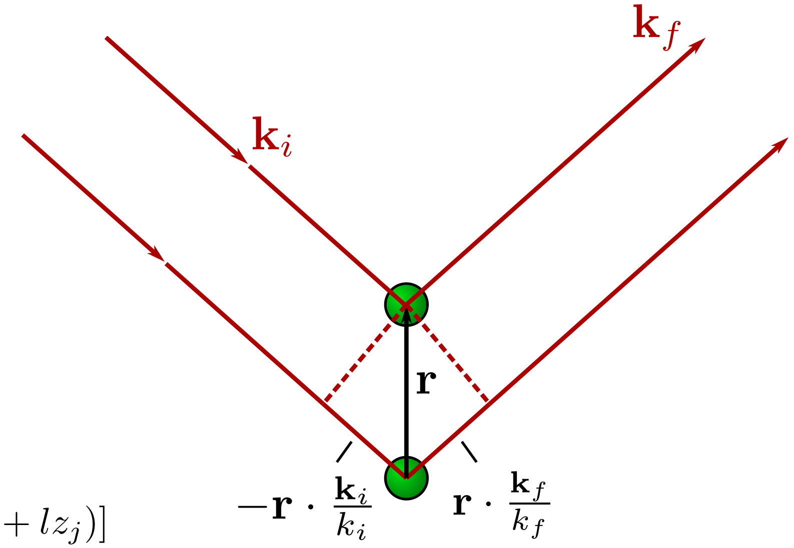

Structure factor *F(hkl)* is the Fourier transform of the unit cell scattering potential.

Scattering from a unit cell

Magnetic structure factor

The magnetic structure factor is obtained in the same way, but it is also proportional to the magnetic moment of the involved atoms ⟶ directional dependence, $\mathbf{F}_M$ is a vector

$$\mathbf{F}_M(hkl) = \sum_j \boldsymbol{\mu}_j f_j(\mathbf{k}) \exp(i\mathbf{k}\mathbf{r}_j) = \sum_j \boldsymbol{\mu}_j f_j(\mathbf{k}) \exp\left[2\pi i(hx_j + ky_j + lz_j)\right]$$

Only the component of $\mathbf{F}_M$ which is perpendicular to $\mathbf{k}$ contributes to magnetic scattering:

$$\mathbf{Q}_M = \hat{\mathbf{k}} \times (\mathbf{F}_M \times \hat{\mathbf{k}})$$

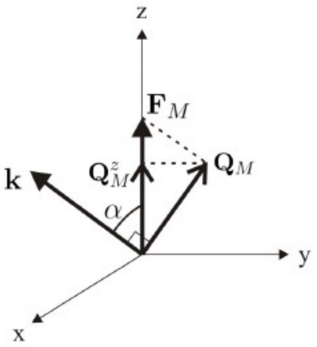

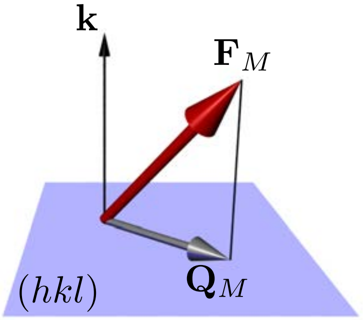

Equivalent: Projection of $\mathbf{F}_M$ onto *(hkl)* plane

Scattering from a unit cell

Example: Ferromagnetic structure

$$\mathbf{F}_M(hkl) = \sum_j \boldsymbol{\mu}_j f_j(\mathbf{k}) \exp(i\mathbf{k}\mathbf{r}_j) = \sum_j \boldsymbol{\mu}_j f_j(\mathbf{k}) \exp\left[2\pi i(hx_j + ky_j + lz_j)\right]$$

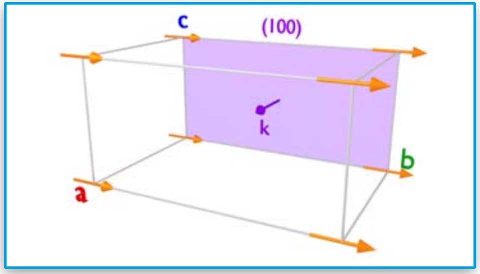

$$\mathbf{F}_M(100) = \begin{pmatrix} 0 \\ \mu \\ 0 \end{pmatrix} f(\mathbf{k})$$

$$\mathbf{Q}_M(100) = \mathbf{F}_M(100)$$

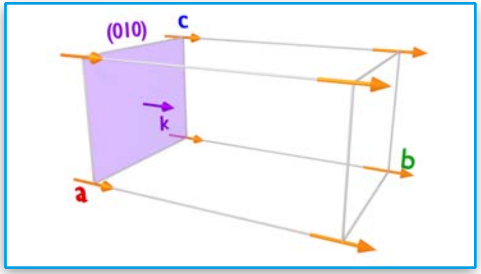

$$\mathbf{F}_M(010) = \begin{pmatrix} 0 \\ \mu \\ 0 \end{pmatrix} f(\mathbf{k})$$

$$\mathbf{Q}_M(010) = 0$$

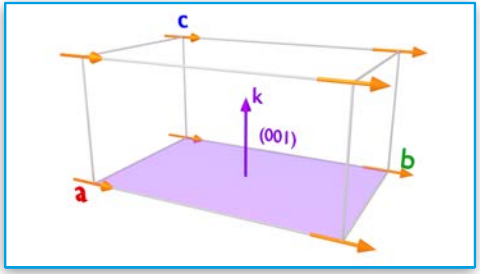

$$\mathbf{F}_M(001) = \begin{pmatrix} 0 \\ \mu \\ 0 \end{pmatrix} f(\mathbf{k})$$

$$\mathbf{Q}_M(001) = \mathbf{F}_M(001)$$

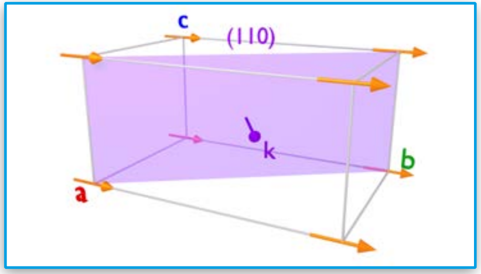

$$\mathbf{F}_M(110) = \begin{pmatrix} 0 \\ \mu \\ 0 \end{pmatrix} f(\mathbf{k})$$

$$\mathbf{Q}_M(110) = \mathbf{F}_M(110) \sin\alpha$$

Experimental procedure

Basic diffractometer (constant wavelength)

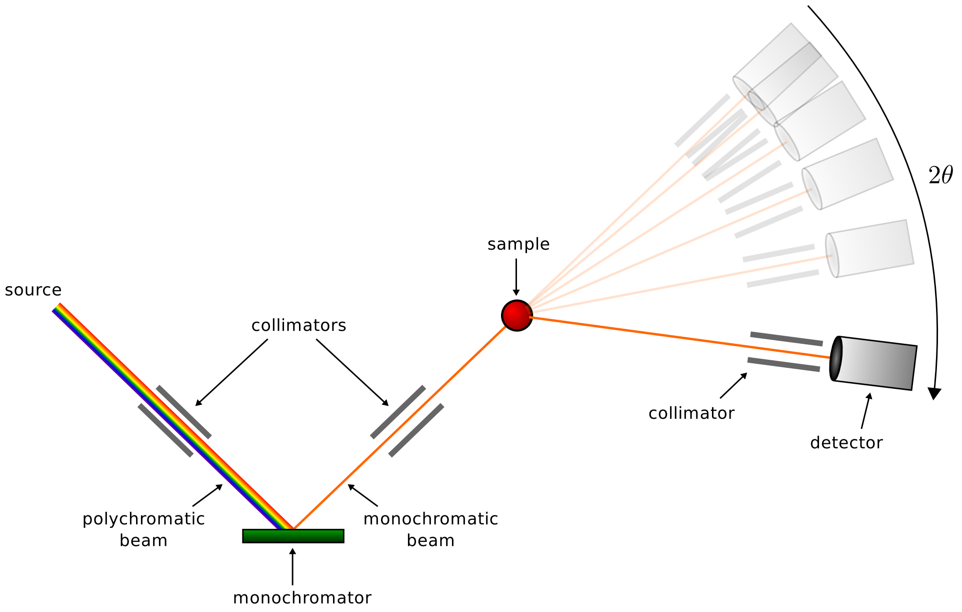

Experimental procedure

Basic diffractometer (constant wavelength)

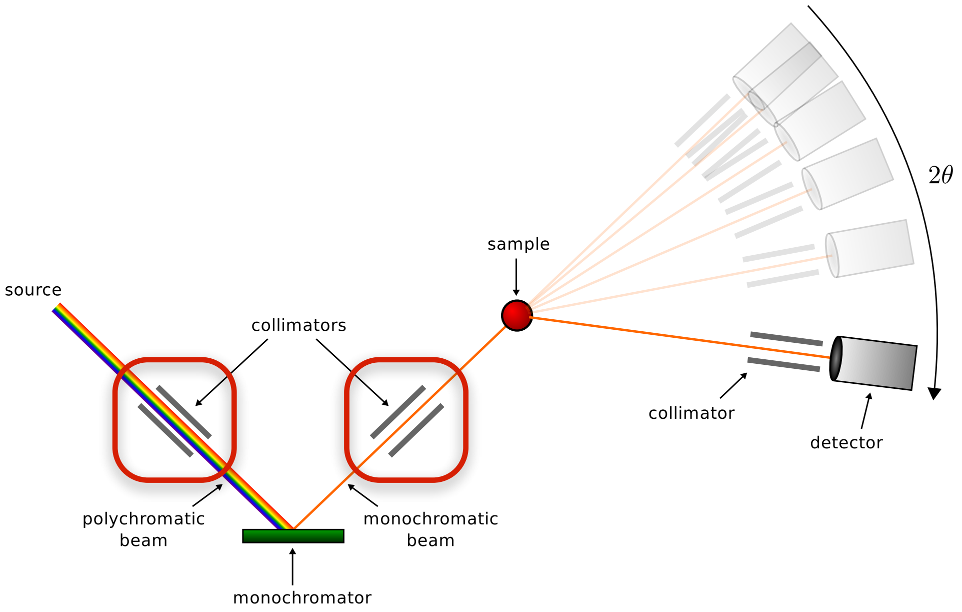

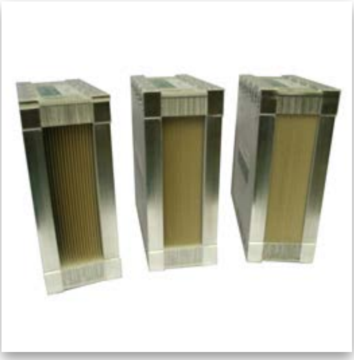

collimator

defines the beam shape and divergence

Soller collimators, slits

Experimental procedure

Basic diffractometer (constant wavelength)

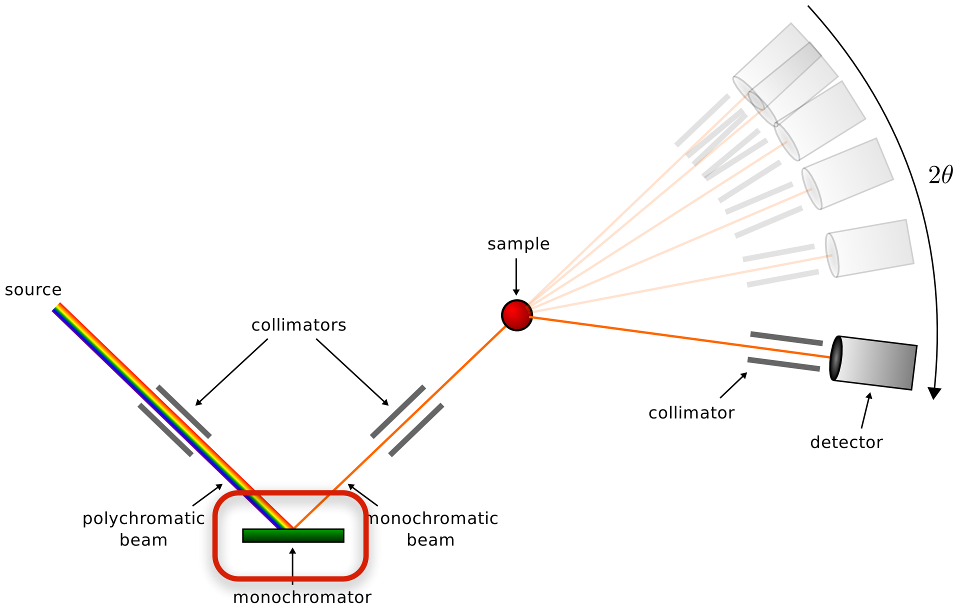

monochromator

(assembly of) high quality single crystals

choice of wavelength and resolution

typically Cu, Ge, HOPG, Si

diffracts also higher harmonics $\lambda/2$, $\lambda/3$, ...

$$n\lambda = 2d \sin\theta$$

Experimental procedure

Basic diffractometer (constant wavelength)

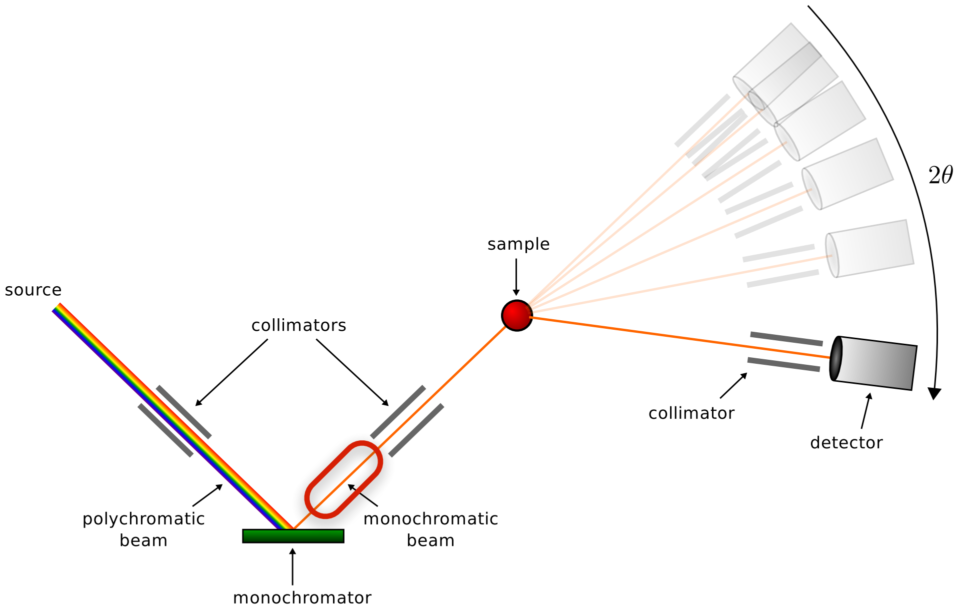

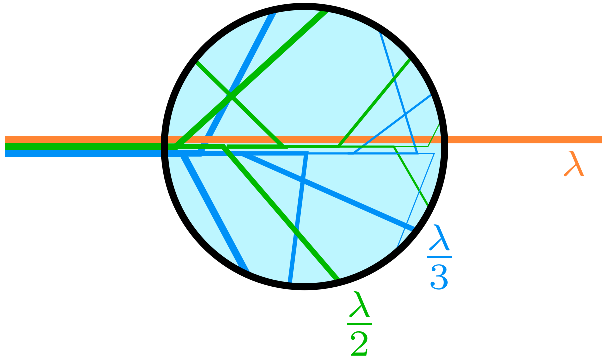

filter

diffracts shorter λ out of the beam

$\lambda/2d_{Filter}>1$

typically PG, Be, no $\lambda/2$ filter needed for Si, Ge

(111) is used, because (222) is forbidden

Experimental procedure

Basic diffractometer (constant wavelength)

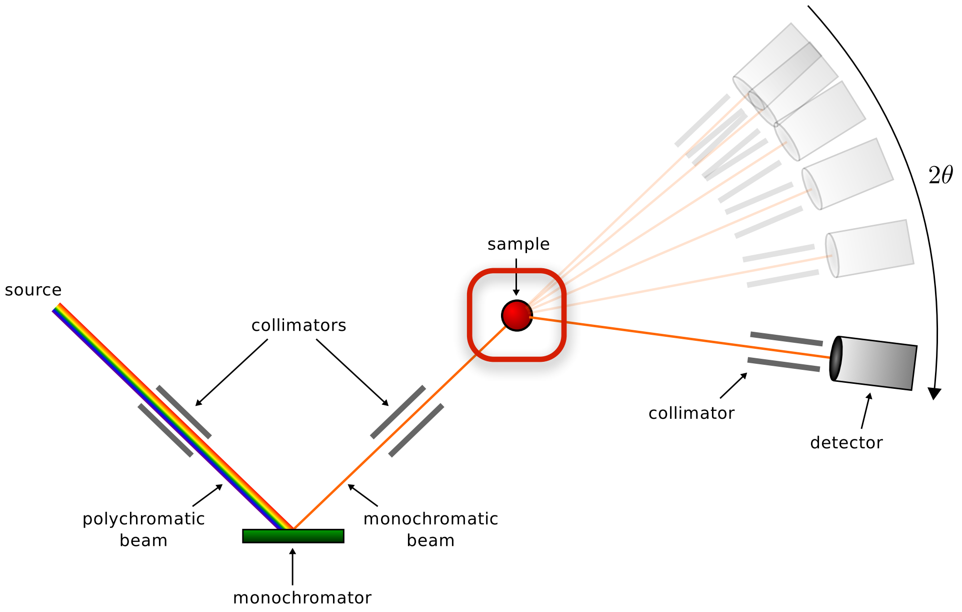

sample environment

cryostat, cryomagnet,
furnace, pressure cell, CryoPAD

Experimental procedure

Basic diffractometer (constant wavelength)

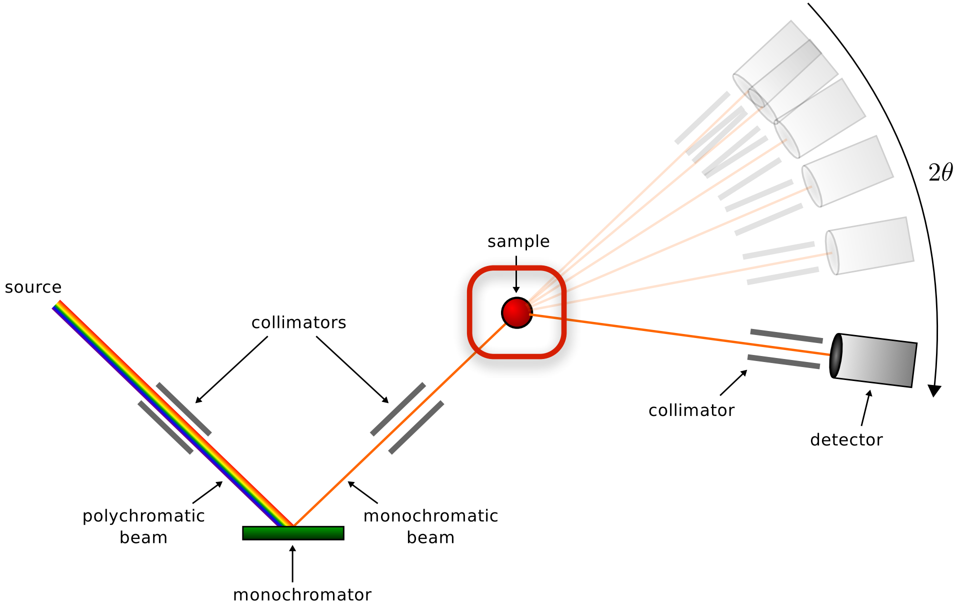

sample environment
cryostat, cryomagnet,
furnace, pressure cell, CryoPAD

Experimental procedure

Basic diffractometer (constant wavelength)

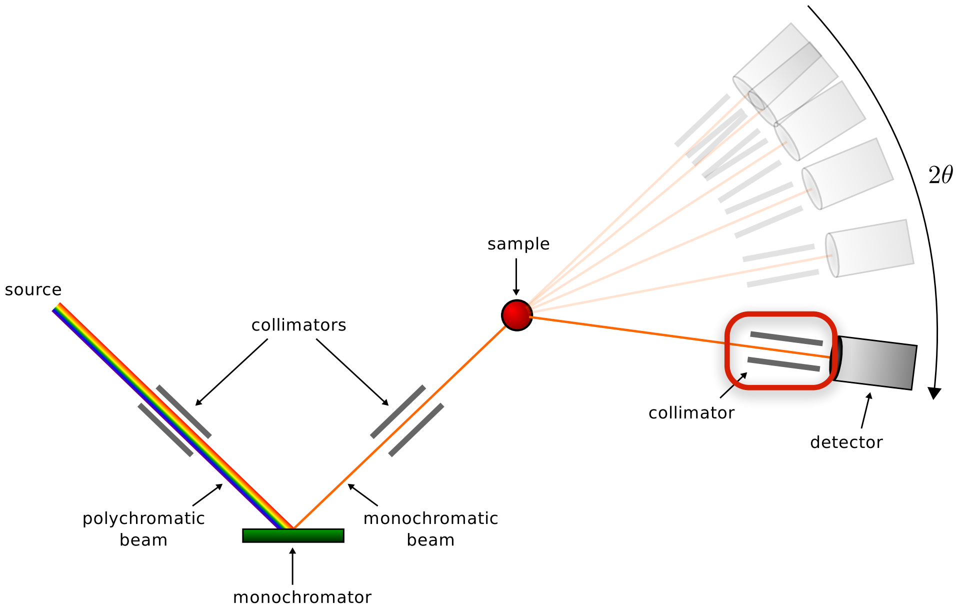

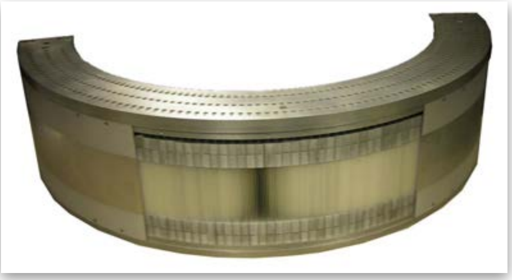

collimator

e.g. radial oscillating collimator
reduces background from sample environment
or another Soller collimator to
increase resolution

Experimental procedure

Basic diffractometer (constant wavelength)

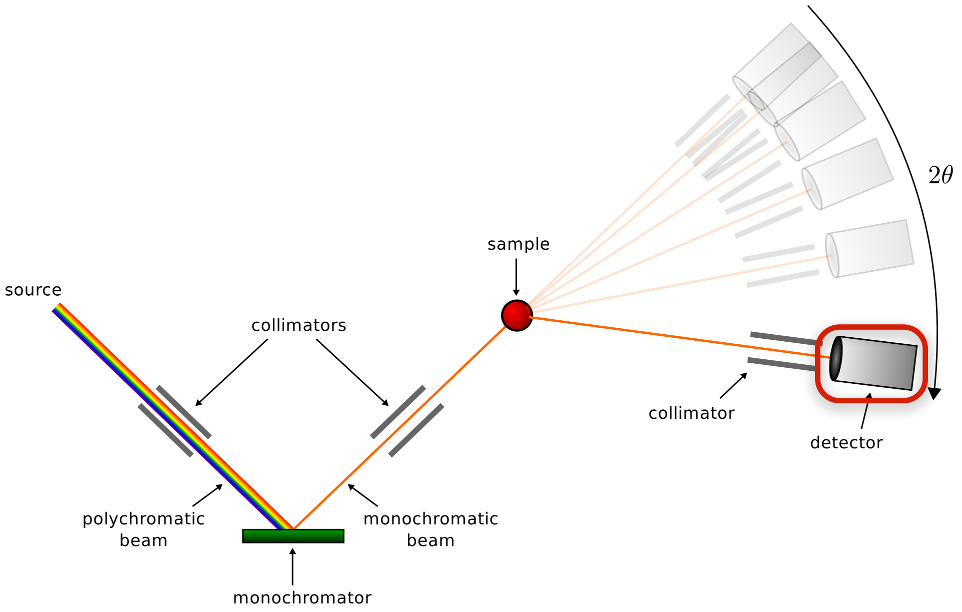

detector

gas cells in which an incoming neutron triggers a nuclear reaction producing a charged particle which then is detected typically ^{3}He or B_3F

Experimental procedure

Time-of-flight diffractometer (polychromatic)

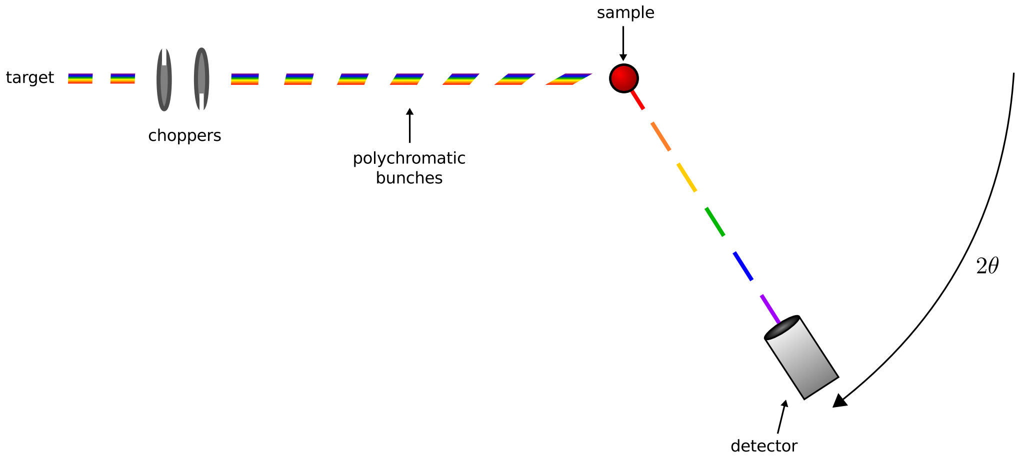

chopper

defines the wavelength band

avoids frame overlap

Experimental procedure

Time-of-flight diffractometer (polychromatic)

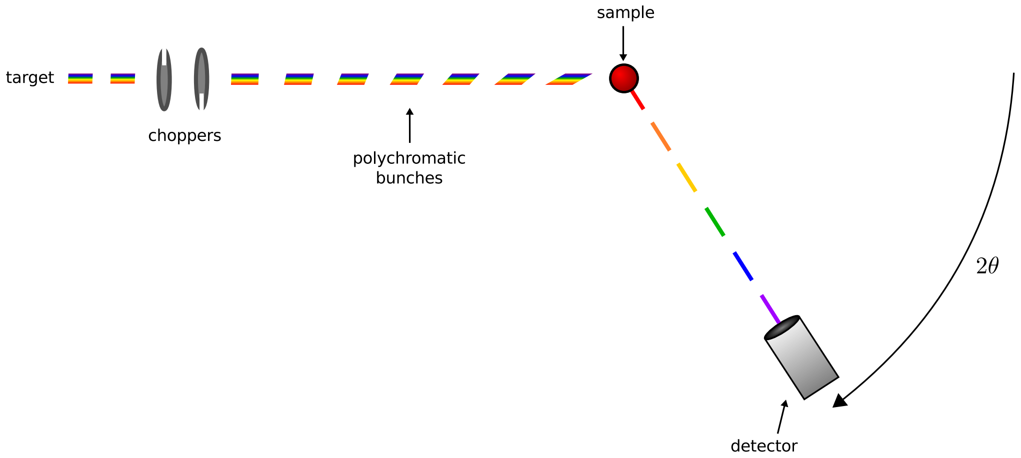

time of flight of the neutrons is related to the their wavelength

$$t = \frac{m_n}{h} \lambda L$$

diffraction pattern is recorded at constant scattering angle
(close to 180° for best resolution, small Δt/t)

$$\frac{\Delta\lambda}{\lambda} = \Delta\theta_M \cot\theta_M$$

Experimental procedure

Powder diffraction

D20 (high flux)

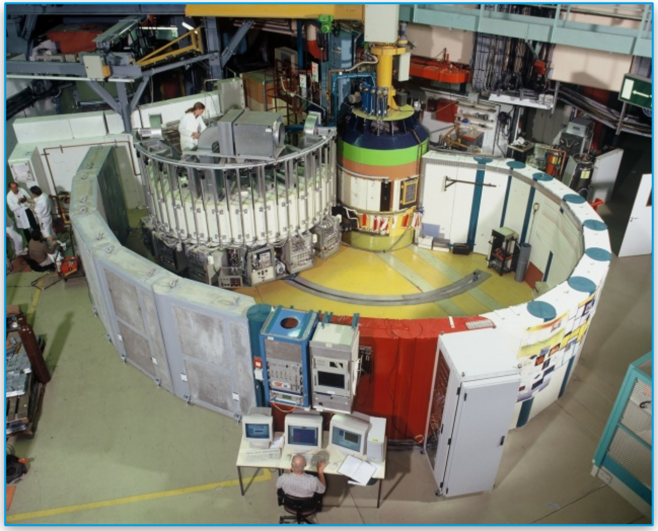

sample in a vanadium container

V scatters only incoherently

Experimental procedure

Powder diffraction

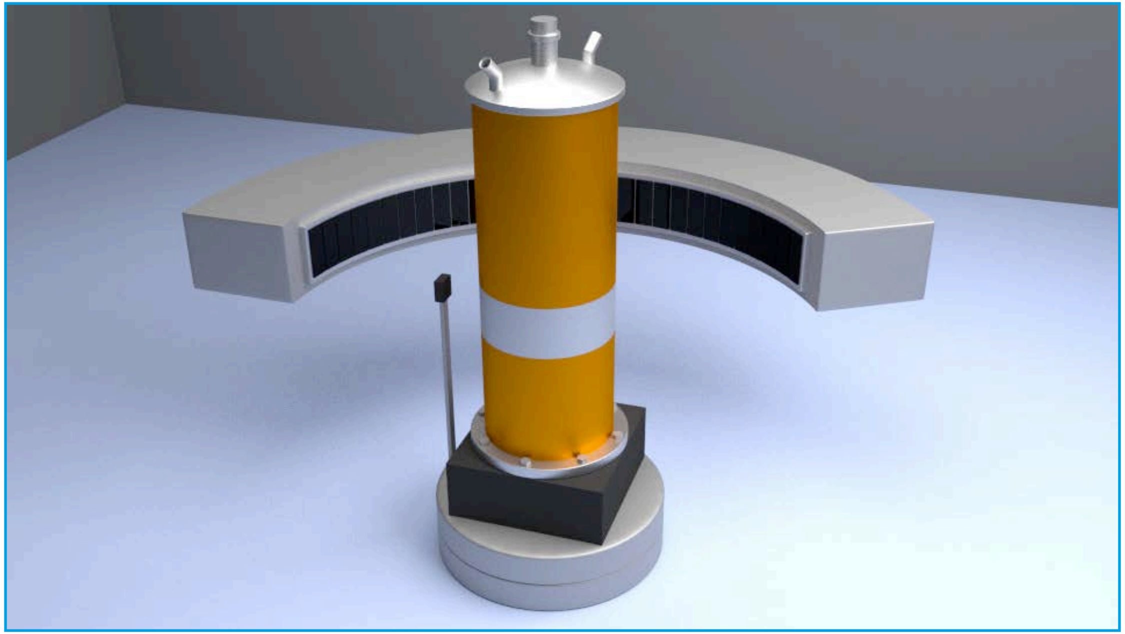

Experimental procedure

Powder diffraction

Result: Diffraction pattern

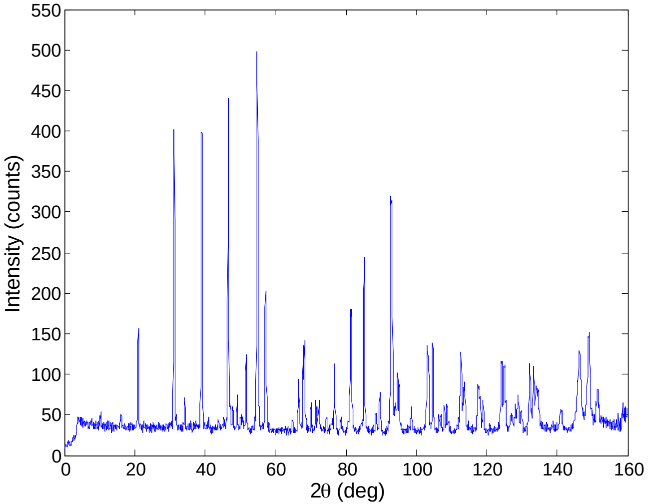

Useful information lies in the

- position
- the intensity
- the shape and width

of the reflections.

Experimental procedure

Powder diffraction

1. Position

Bragg's law $n\lambda = 2d\sin\theta$

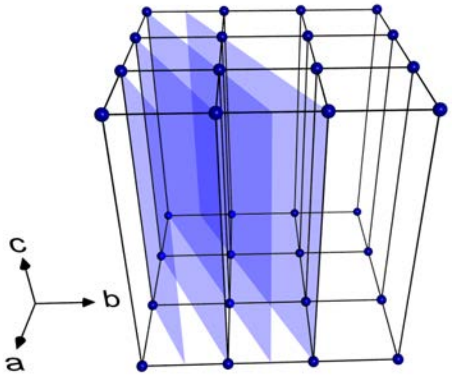

monoclinic

$$d = \left(\frac{h^2}{a^2\sin^2\beta} + \frac{k^2}{b^2} + \frac{l^2}{c^2\sin^2\beta} - \frac{2hl\cos\beta}{ac\sin^2\beta}\right)^{-\frac{1}{2}}$$

orthorhombic

$$d = \left(\frac{h^2}{a^2} + \frac{k^2}{b^2} + \frac{l^2}{c^2}\right)^{-\frac{1}{2}}$$

cubic

$$d = a(h^2 + k^2 + l^2)^{-\frac{1}{2}}$$

with θ and λ known → able to obtain lattice parameters and propagation vectors

Magnetic Bragg reflections can be found at $\mathbf{k} = \mathbf{G} \pm \mathbf{q} \longrightarrow$ $d = a\left[(h+q_x)^2 + (k+q_y)^2 + (l+q_z)^2\right]^{-\frac{1}{2}}$

Experimental procedure

Powder diffraction

2. Intensity $I \sim F^2$

nuclear structure factor
(interaction between neutron and core potential of nuclei)

$$F_N(\mathbf{k}) = \sum_j b_j \exp(i\mathbf{k}\mathbf{r}_j) \exp\left(-B_j \frac{\sin^2\theta}{\lambda^2}\right)$$

magnetic structure factor
(interaction between neutron and electron's magnetic field)

$$F_M(\mathbf{k}) = \sum_j \boldsymbol{\mu}_j f_j(\mathbf{k}) \exp(i\mathbf{k}\mathbf{r}_j) \exp\left(-B_j \frac{\sin^2\theta}{\lambda^2}\right)$$

magnetic form factor

$$f(\mathbf{k}) = \int_{-\infty}^{\infty} \rho_{mag}(\mathbf{r}) \exp(i\mathbf{k}\mathbf{r}) d\mathbf{r}$$

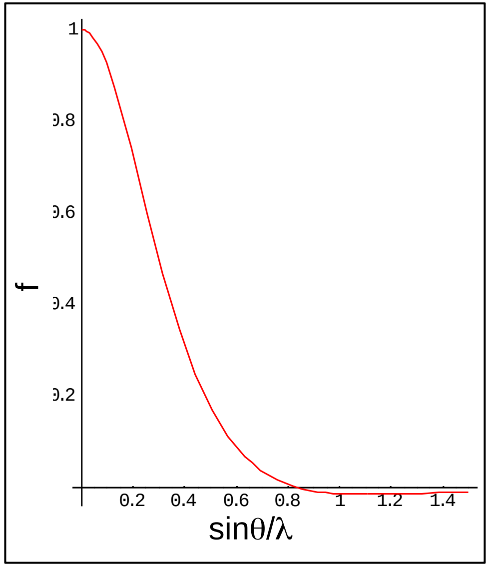

Experimental procedure

Powder diffraction

3. Peak width and shape

source, monochromator, slits, collimators, sample strain, stress, correlation length etc. have an influence on the peak shape and the peak width

Caglioti formula

$$\mathrm{FWHM}^2 = u\tan^2\theta + v\tan\theta + w$$

resolution function minimum at the take-off angle $2\theta_M$

(focussing effect)

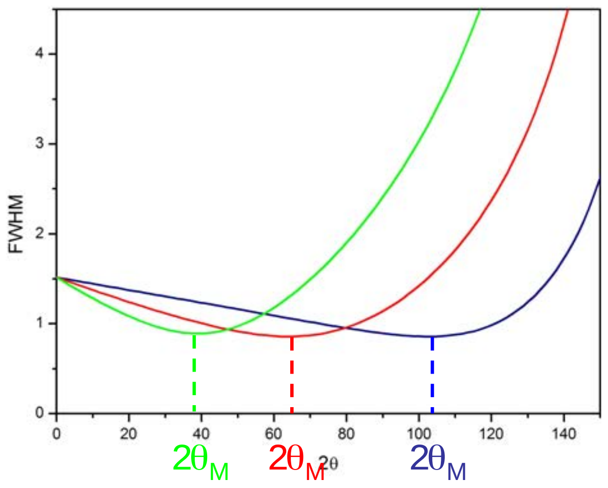

Experimental procedure

Powder diffraction

Thermodiffraction

Collection of diffraction patterns as a function of temperature.
Clearly reveals structural and magnetic phase transitions.

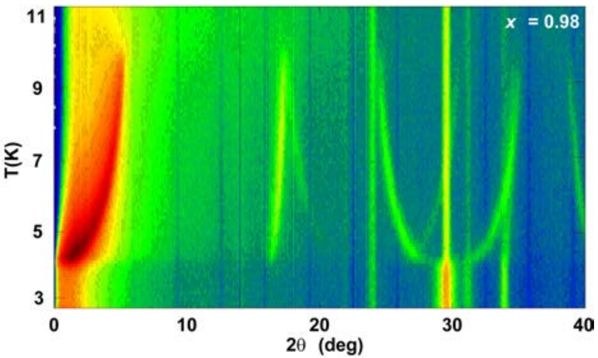

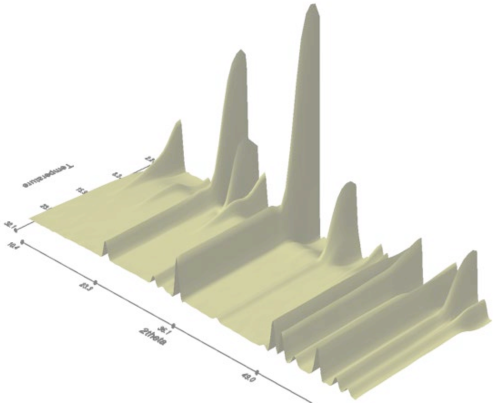

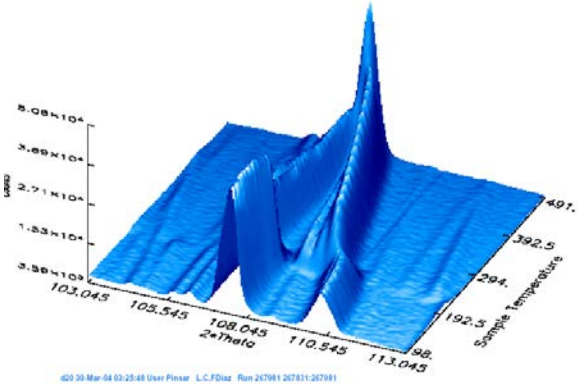

Experimental procedure

Single crystal diffraction - 4-circle geometry

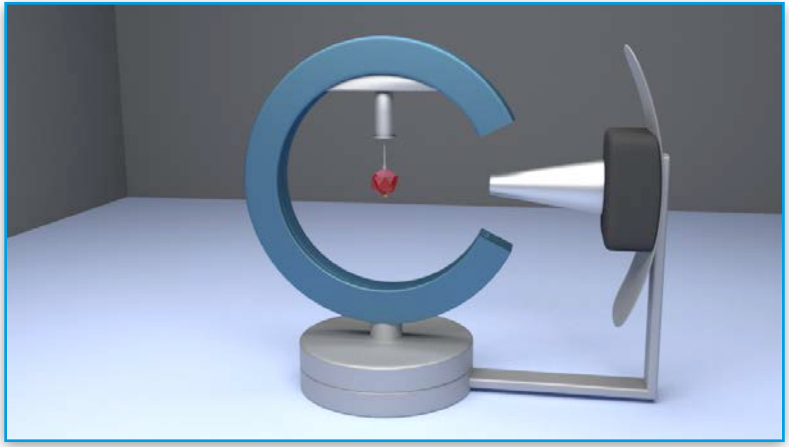

by adjusting 2θ, ω, χ and ϕ

the sample is put in reflection position

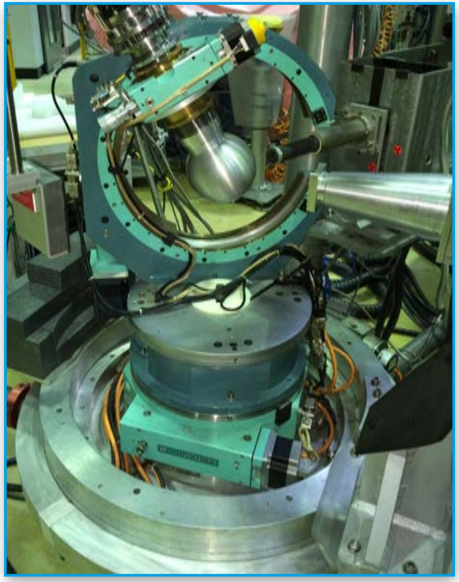

D10 (ILL)

single crystal on Al pin

Experimental procedure

Single crystal diffraction - Normal beam geometry

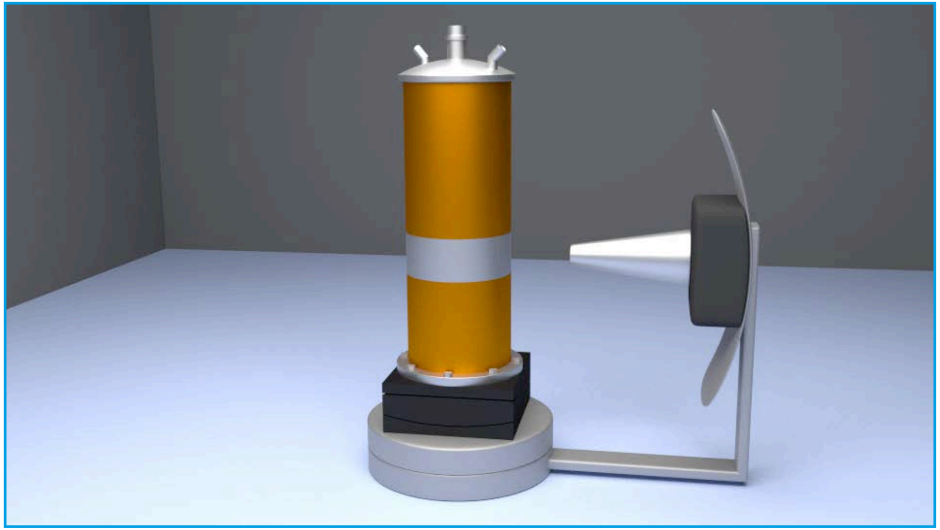

cryomagnets, pressure cells, ...
cannot be tilted much

→ confined to the scattering plane
e.g. only (*hk*0) reflections

→ lifting counter
able to reach *l*=1, 2...

Experimental procedure

Single crystal diffraction - Laue method

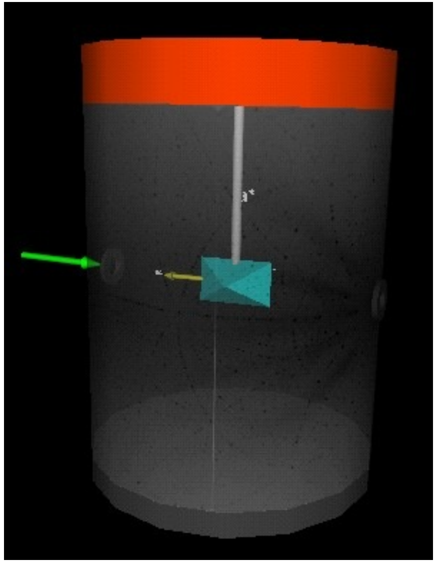

polychromatic beam

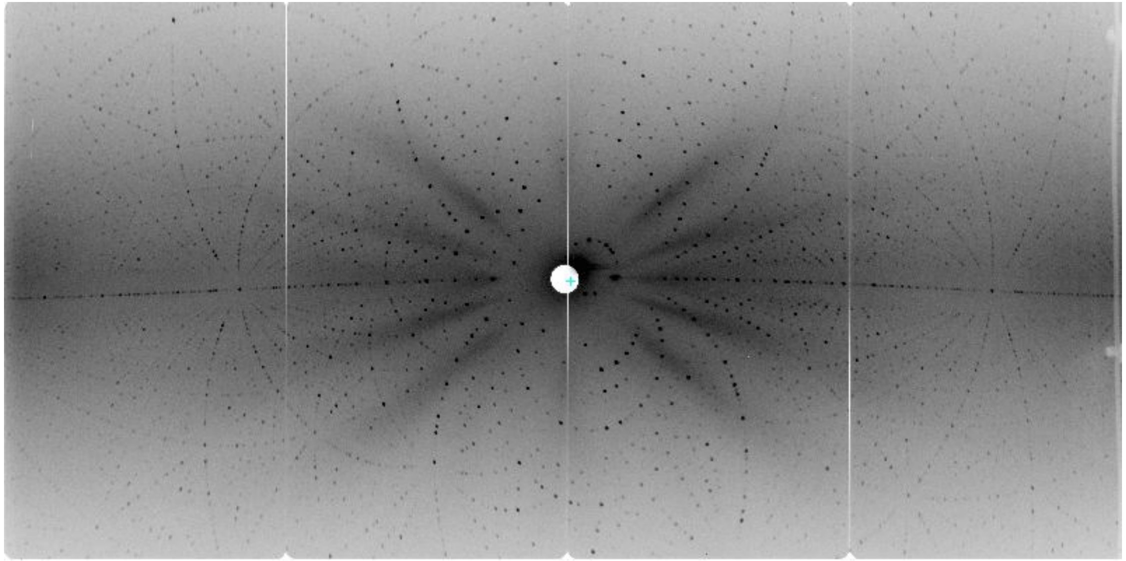

→ every accessible *hkl* plane is in reflection position
for a particular wavelength

Experimental procedure

Single crystal diffraction - Laue method

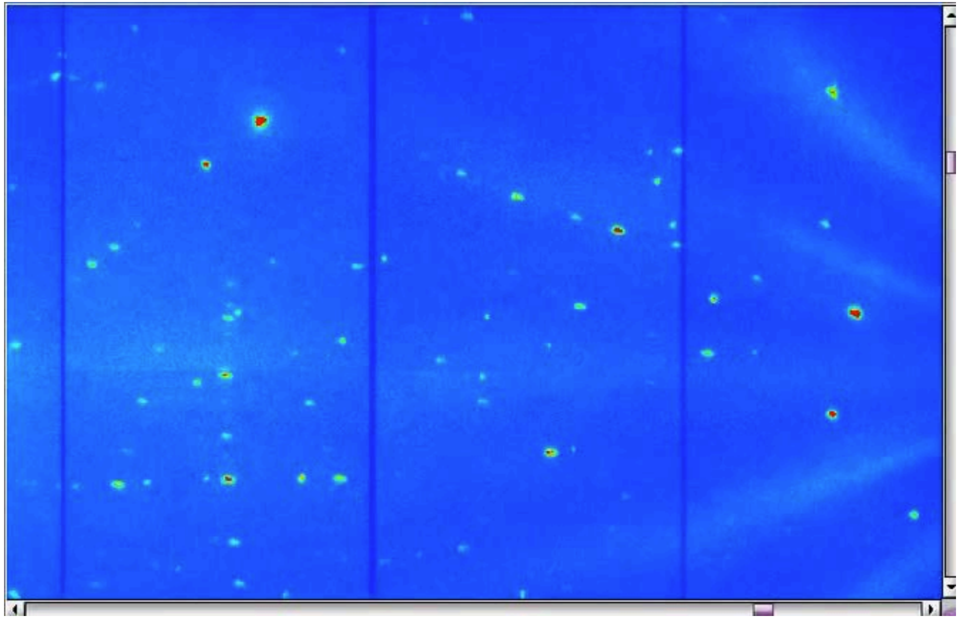

- quickly orient single crystals
- observe phase transitions
- magnetic satellites
- find propagation vectors
- structure analysis also possible

Summary

Diffraction from magnetic materials

- magnetic scattering is comparable in intensity to nuclear scattering
- Only the component of the magnetic moment perpendicular to the scattering vector is measurable
- The magnetic form factor is the Fourier transform of the atomic magnetisation density
- The magnetic structure factor is the Fourier transform of the unit cell magnetisation density
- We measure $I \sim F^2$ $\longrightarrow$ phase information is lost $\longrightarrow$ models necessary
- How dow we get those models? See you tomorrow

NEUTRONS FOR SOCIETY

I N S T I T U T   L A U E   L A N G E V I N